A. P. Alexandrov
RESEARCH INSTITUTE
OF TECHNOLOGY
N I T I

Phase Diagrams for Multicomponent Systems Containing Corium and Products of its Interaction with NPP Materials
(CORPHAD)
Phase 2

Investigation of binary oxidic systems: UO_2–SiO_2 system

Progress report
01/05/06 – 30/11/06

Project title	Phase Diagrams for Multicomponent Systems Containing Corium and Products of its Interaction with NPP Materials (CORPHAD, Phase 2), No.1950.2
Commissioned by	ISTC
File code	CORPHAD/RCP-0602
Implementing organization	The Alexandrov Research Institute of Technology (NITI) of the Atomic Energy Agency of the Russian Federation 188540, Sosnovy Bor, Leningrad Region, NITI, Russia
Project manager	Name: Yu. N. Aniskevich Signature
	Date: November 2006

Авторы

Dr., Corr.Mem. RAS	V.V. Gusarov
Ph.D.	L.P. Mezentseva
	V.F. Popova
	V. I. Almyashev
	N.A. Lomanova
	S.K. Kuchayeva
Dr., Prof..	V.B. Khabensky
Dr.	S.V. Bechta
Ph.D.	V.S. Granovsky
	S.A. Vitol
	E.V. Krushinov
Ph.D.	S.Yu. Kotova
	V.G. Blisnyk
	E.K. Kalyago
	A.V. Lysenko
	V.R. Bulygin
	E.V. Shevchenko
	N.E. Kamensky
	R.A. Kosarevsky
	V.V. Martynov
	E.M. Belyaeva
Ph.D.	A.A. Sulatsky
Translated by:	S.V. Shuvalov

CONTENTS

Introduction

During the ex-vessel stage of a severe nuclear reactor accident, molten corium may contain a significant amount of iron oxides (products of steel oxidation) and silicon oxides (products of corium interaction with concretes, sacrificial material and refractories).

The said circumstance dictates a necessity of investigating the silicon oxide-containing systems for optimizing the available databases and verifying numerical codes. In accordance with the Work Plan for CORPHAD, Phase 2, the interaction of components within the UO_2–SiO_2 system has been investigated in an inert atmosphere.

The published sources offer two phase diagrams of the UO_2–SiO_2 system [1, 2], the first of which (Fig. 1) is a simple eutectic diagram (1650±10°C), while the second one (Fig. 2) shows the presence of a segregation area, about 20 mol. % wide, above the monotectic temperature (2070±10°C).

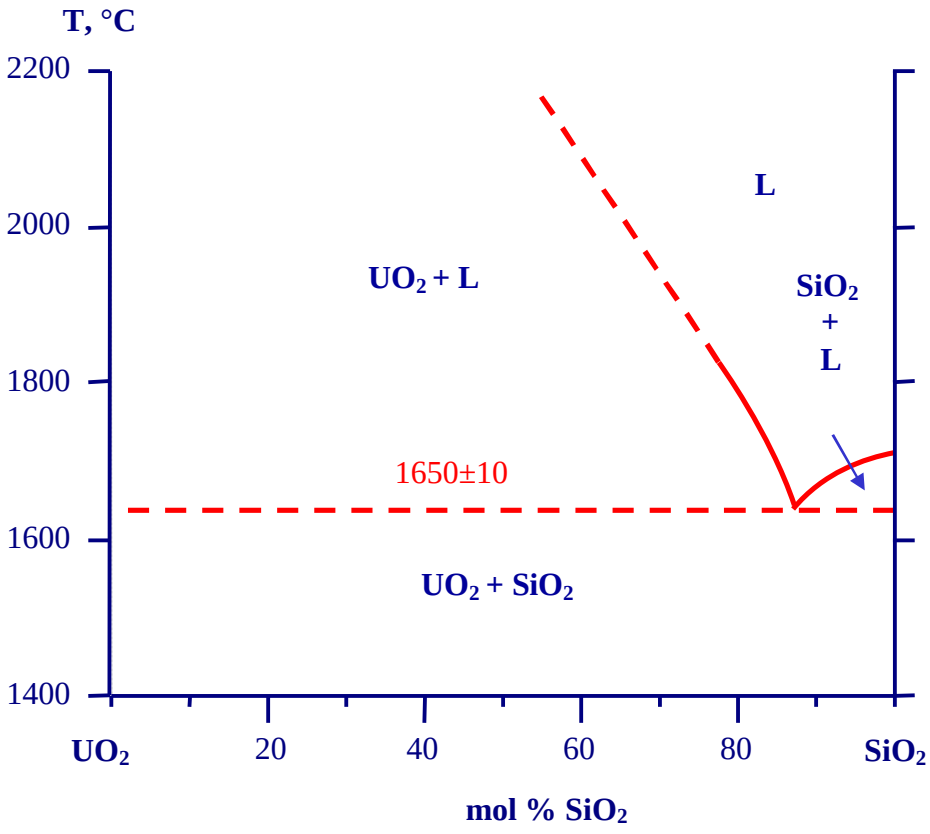

Fig. 1. Phase diagram of the UO_2–SiO_2 system according to S.M. Lang [1]

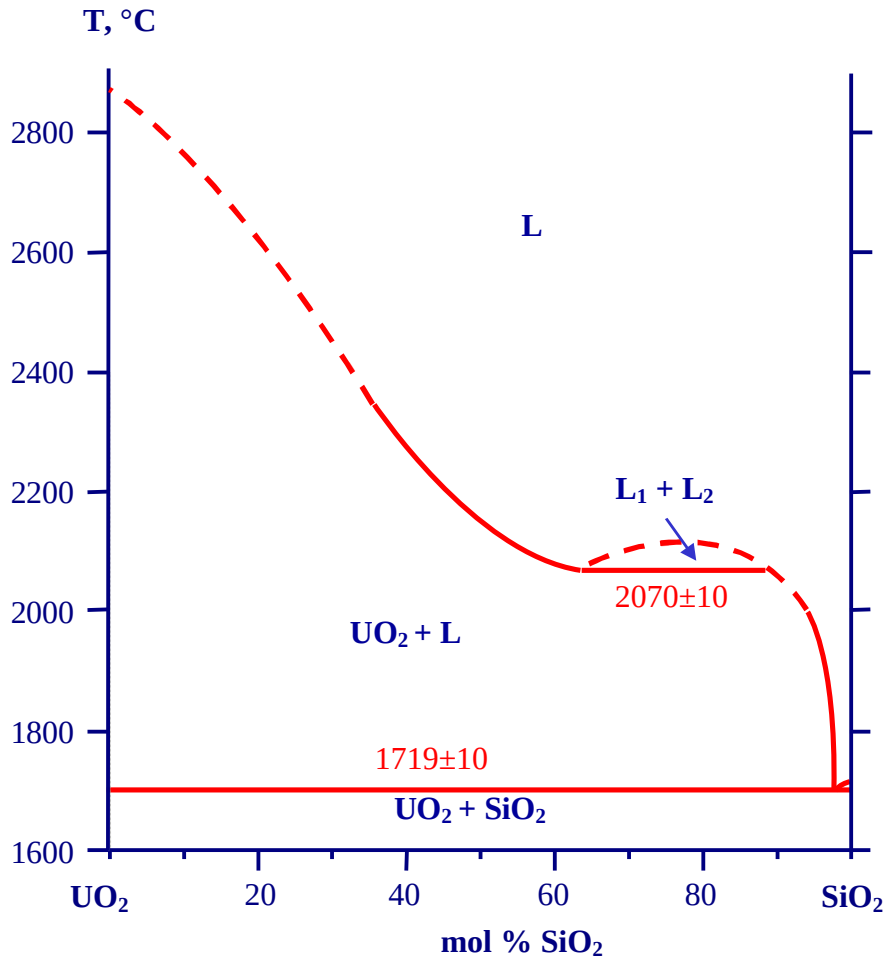

Fig. 2. Phase diagram of the UO_2–SiO_2 system according to S.N. Lung [2]

The arising questions are: which of the given diagrams reflects correctly the interaction of components in the system at high temperatures; does there exist the immiscibility area, and if yes, then which temperature does it exceed and how wide it is.

1. Experimental part

2.1. Materials used, specimens preparation and investigation techniques

The initial materials used for investigating the UO_2–SiO_2 system were reagents with a high degree of purity: 99.00 % pure UO_2 and 99.99% pure SiO_2.

The charge was produced by components grinding and mixing in the vibratory mill in air within 2 h. Then the obtained mixture was dried in the drying box at 120°C for 30 min, and at 20°C within 8 h. A part of the mixture taken by quartering was subjected to XRF for analyzing the prepared mix. The charge was found to contain (in mass %) 49.3 SiO_2 – 50.7 UO_2.

The tests were performed using an original facility – the Galakhov microfurnace [3] designed and manufactured at the I.V. Grebenschikov ISC of RAS and modernized at the A.P. Alexandrov NITI (Fig. 3).

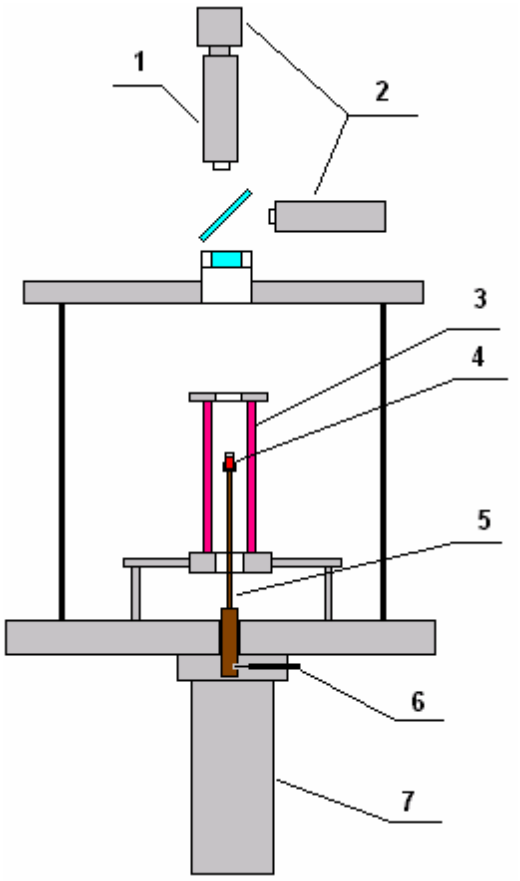

1. Pyrometer. 2. Video cameras. 3. Wolfram tubular heater. 4. Molybdenum crucible. 5. Molybdenum specimen holder. 6 Electromagnetic lock.7. Specimen quenching chamber.

Fig. 3. Modernized Galakhov microfurnace:

For melting the UO_2–SiO_2 system specimens in the Galakhov microfurnace, molybdenum crucibles were used to hold from 50 to 150 mg of the charge. Then the crucibles were placed on the molybdenum holder in the isothermal zone of the tubular heater. The operating range of temperature change in the zone spans from 1300 through 2500°C. The specimen surface temperature in the furnace was measured with the RAYTEK MR1-SC spectral ratio pyrometer with the measurement relative error of 1% (i. e. no less than 25°C).

Procedures of all tests were similar and included:

- Crucible weighing;
- Filling of the crucible with charge and ramming;
- Weighing of the charge-loaded crucible;
- Placing of the crucible in the furnace;
- Furnace vacuumization and filling with the argon-hydrogen mixture (Ar+4.2 vol % H_2) at 3 Bar;
- Switching-on of heating and exposure at 1200°C for 5 min;
- Stepwise heating up to the specified temperature;
- Specimen exposure for 1 min with its subsequent dumping into quenching chamber (7).

- Crucible withdrawal from the chamber after cooling, axial cutting and polished section preparation for SEM/EDX analysis.

Microstructure and elemental composition of the quenched specimens were determined by means of Scanning Electron Microscopy (SEM) and Energy Dispersive X-ray Spectrometry (EDX) using the ABT-55 scanning electron microscope (Japan) equipped with the Link_AN_10000/S85 microprobe attachment (Great Britain).

For each specimen to be analyzed, a spectral characteristic was recorded and used for identifying its integral elemental and phase composition. Quantitative analysis was made by comparing spectrum intensities of the reference specimen (a superpure substance prepared in a special way) and of the investigated specimen. The used reference specimens (U, Si) were part of the standard set supplied with the Link attachment.

The error of U and Si determination did not exceed 0.3 mass %.

2.2. Investigation of the binary system UO_2 – SiO_2 in an inert atmosphere

The investigation was carried out in argon with addition of 4.2 vol. % of hydrogen at the pressure of 3 Bar.

Composition of all initial specimens (= charge composition) was the same in all tests. The initial composition approximately corresponds to the midpoint of segregation in the Lung's diagram (Fig. 2, Tab. 2).

Table 2. Specimens initial composition for investigations in the UO_2–SiO_2 system

Composition of all specimens, %	UO_2	SiO_2
mass	50.70	49.30
mol.	18.62	81.38

All in all, 6 tests were performed with quenching from a different temperature, with the same time of isothermal exposure (GCord2-5, 9) except for the first trial test GCord1. In it, the exposure time was minimal (3 sec), and the specimen cooled down quite naturally, i.e., without quenching. This test was performed to check if the facility is capable of working with the UO_2-SiO_2 system. The main characteristics of the performed tests are summed in Tab. 3.

Table 3. Characteristics of the tests (specimen mass, mass loss, quenching temperature and time of isothermal exposure)

Test GCord	Quenching T, °C	Exposure time, sec	Specimen mass, mg	Mass loss, mg	Mass loss, %
2	2000	60	121.10	2.40	1.98
5	2080	60	151.80	4.25	2.80
3	2140	60	125.00	4.20	3.36
1*	2140	3	57.20	2.60	4.54
4	2200	60	132.35	4.45	3.36
9	2400	60	132.00	7.00	5.30

Note: * - Trial test with short exposure time, without specimen quenching.

The molten specimen in the Galakhov microfurnace (GCord4) is shown in Fig. 4

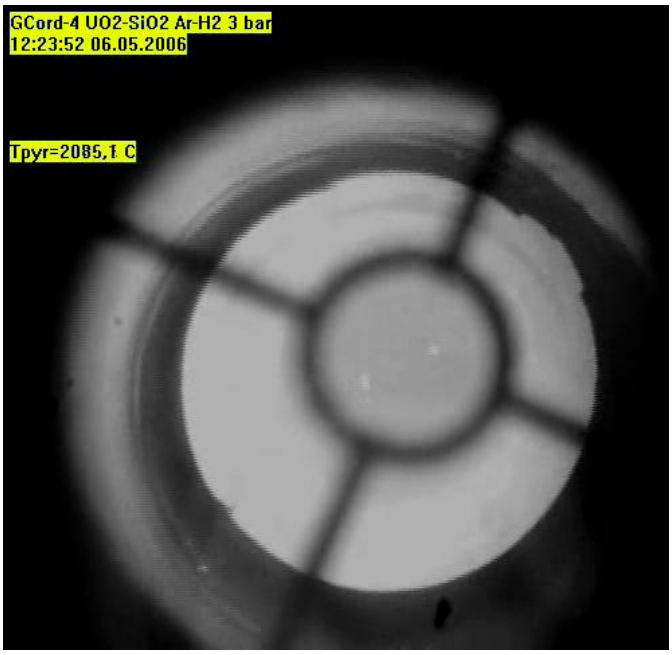

Fig. 4. Molten specimen crucible in the Galakhov microfurnace. Circle in the crosshair corresponds to the pyrometer sighting spot (GCord4).

Thermograms from all tests are given in Figs. 5-10. It should be noted that in test No.2 (Fig. 6) the pyrometer sighting spot was blocked at times when auxiliary operations were performed. The corresponding dips in pyrometer readings do not reflect the specimen surface temperature.

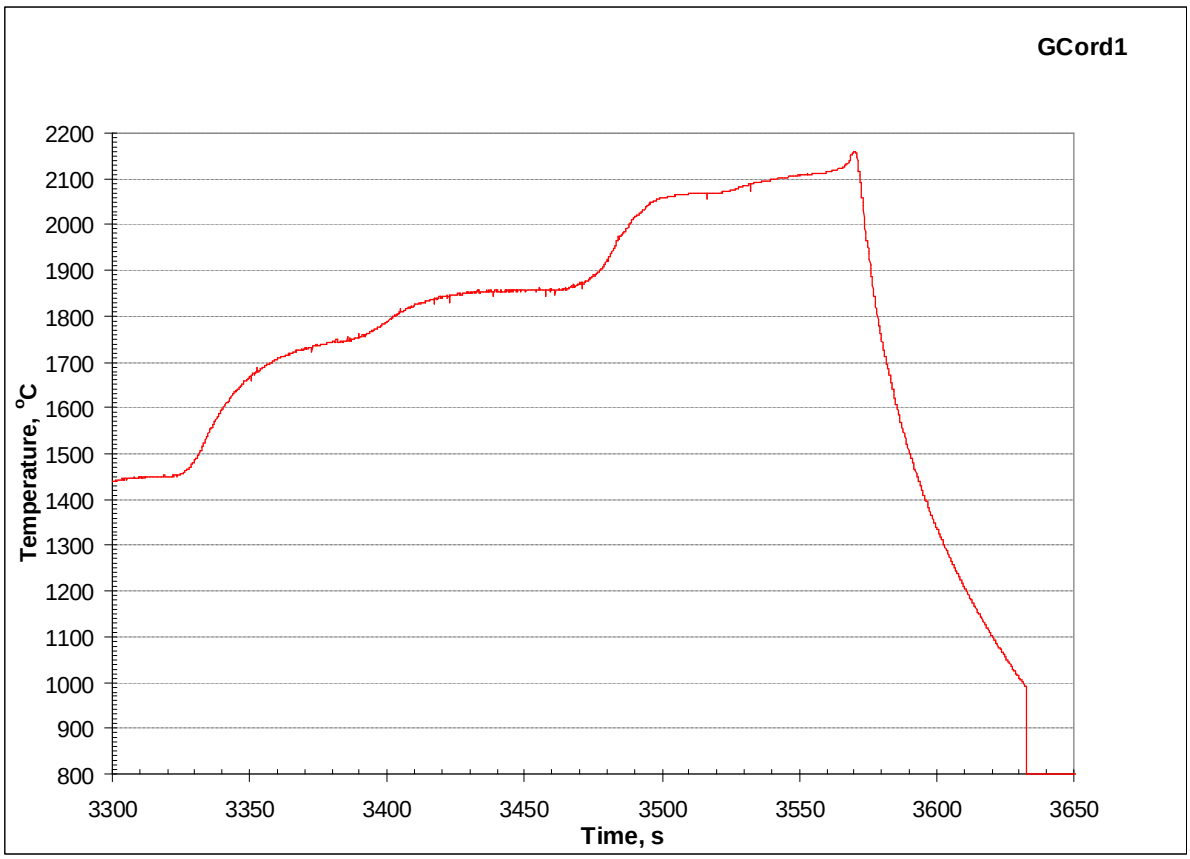

Fig. 5. Thermogram from GCord1

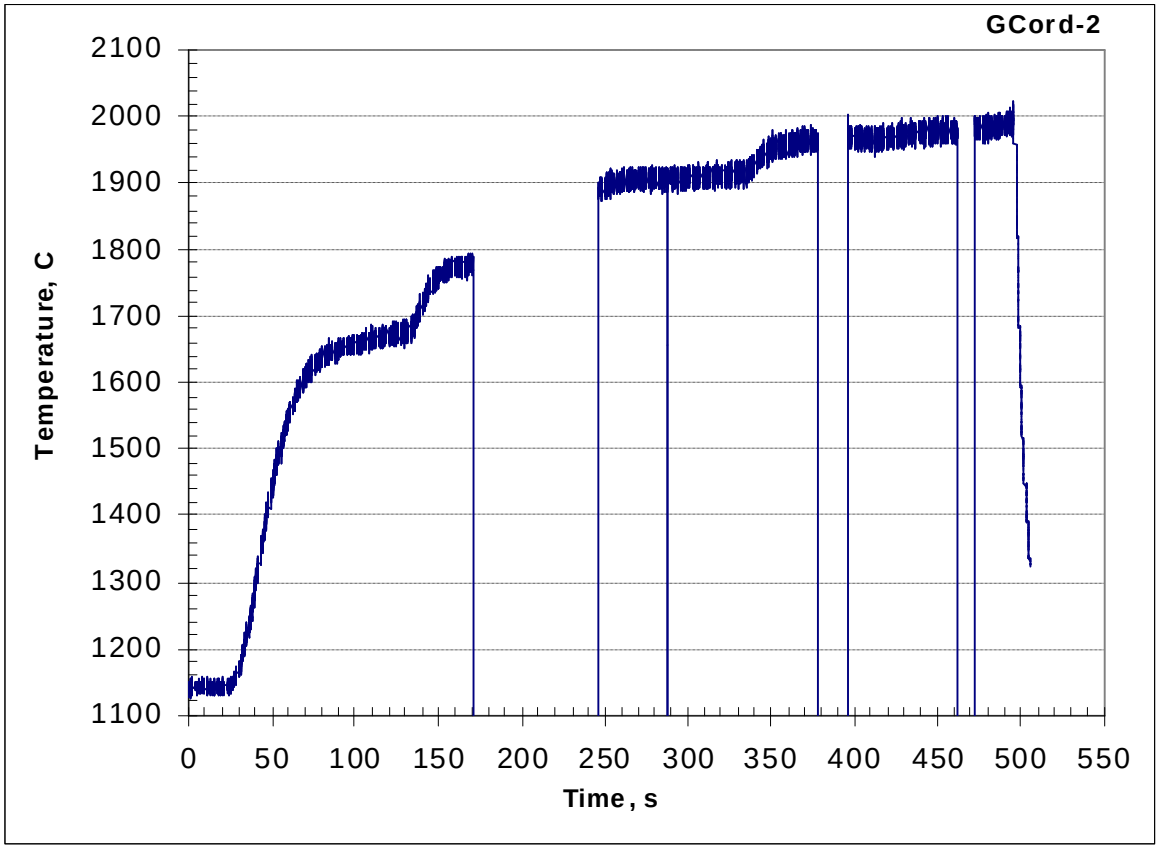

Fig. 6. Thermogram from GCord2

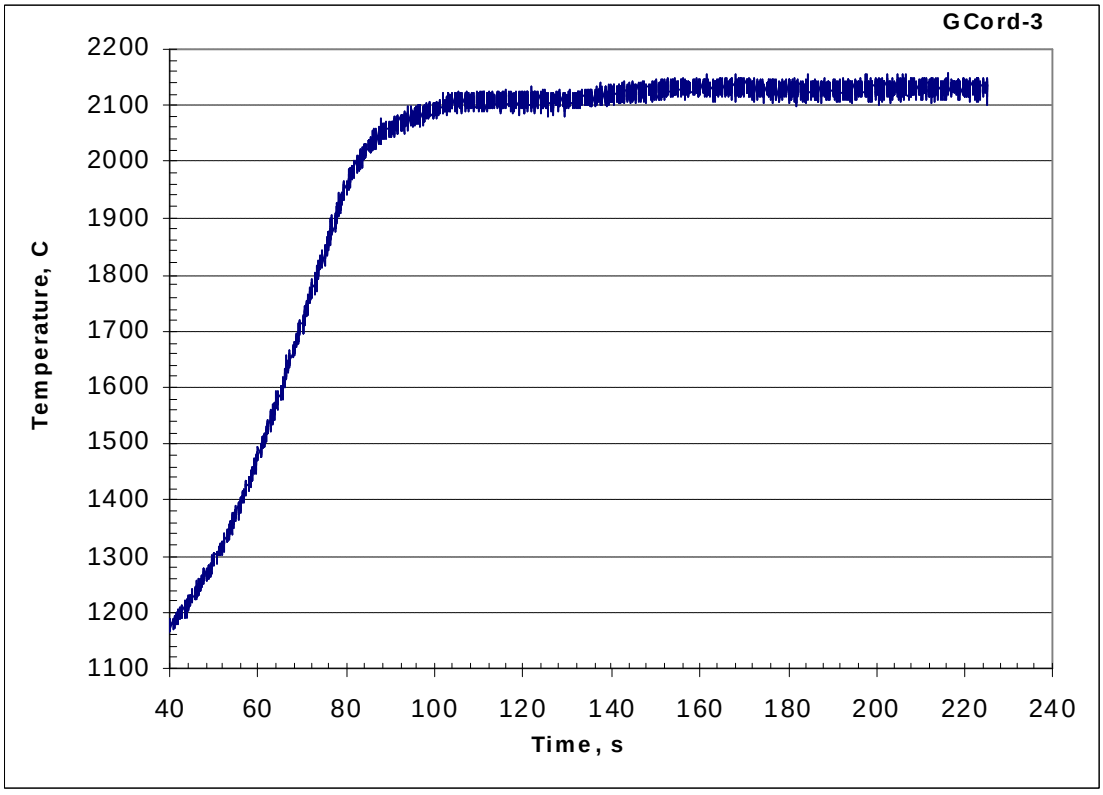

Fig. 7. Thermogram from GCord3

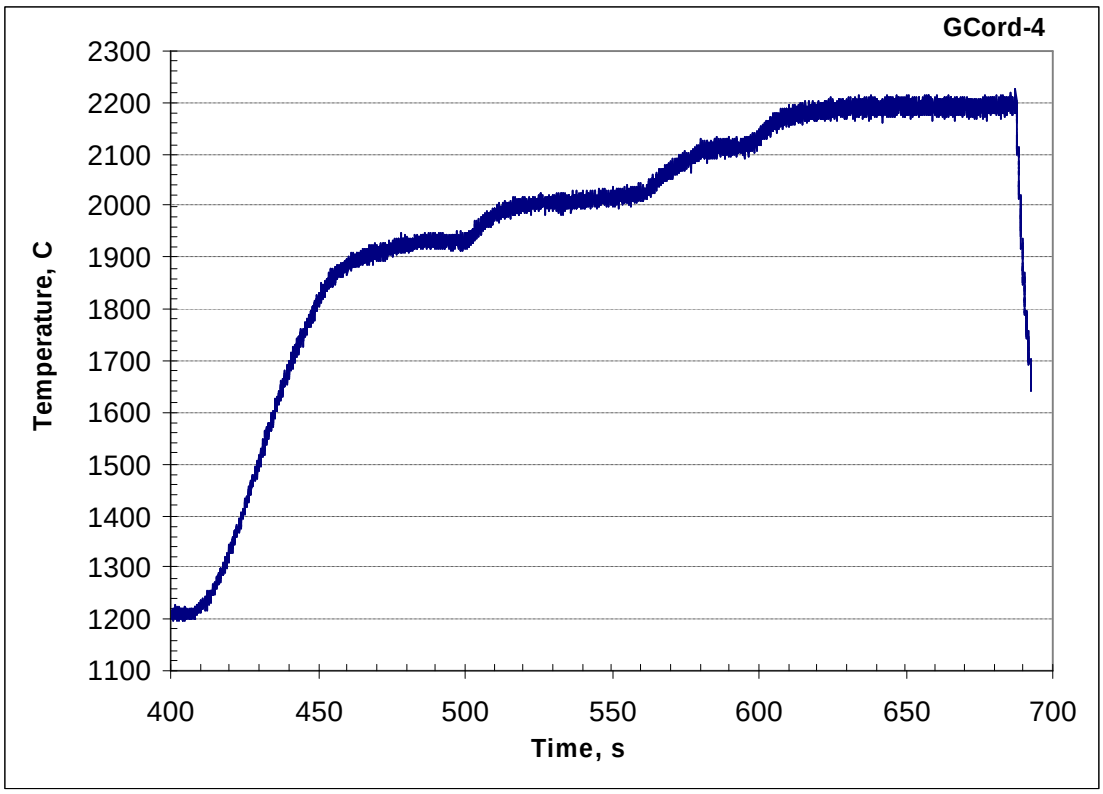

Fig. 8. Thermogram from GCord4

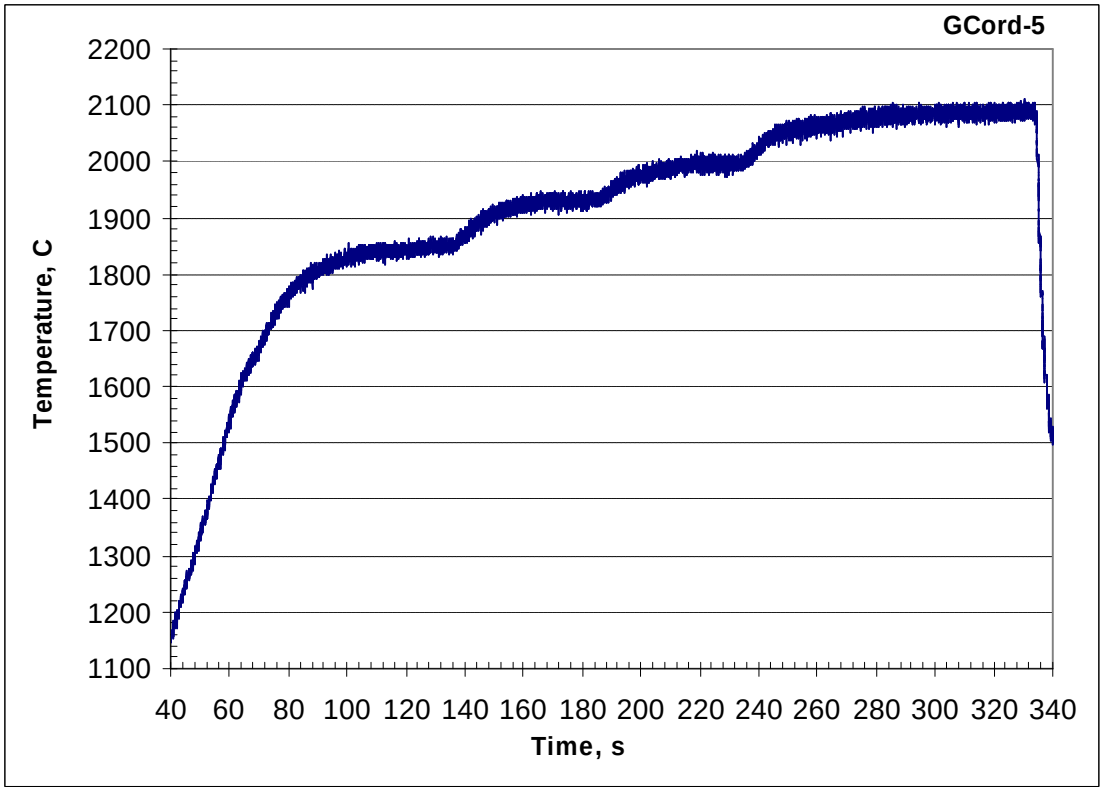

Fig. 9. Thermogram from GCord5

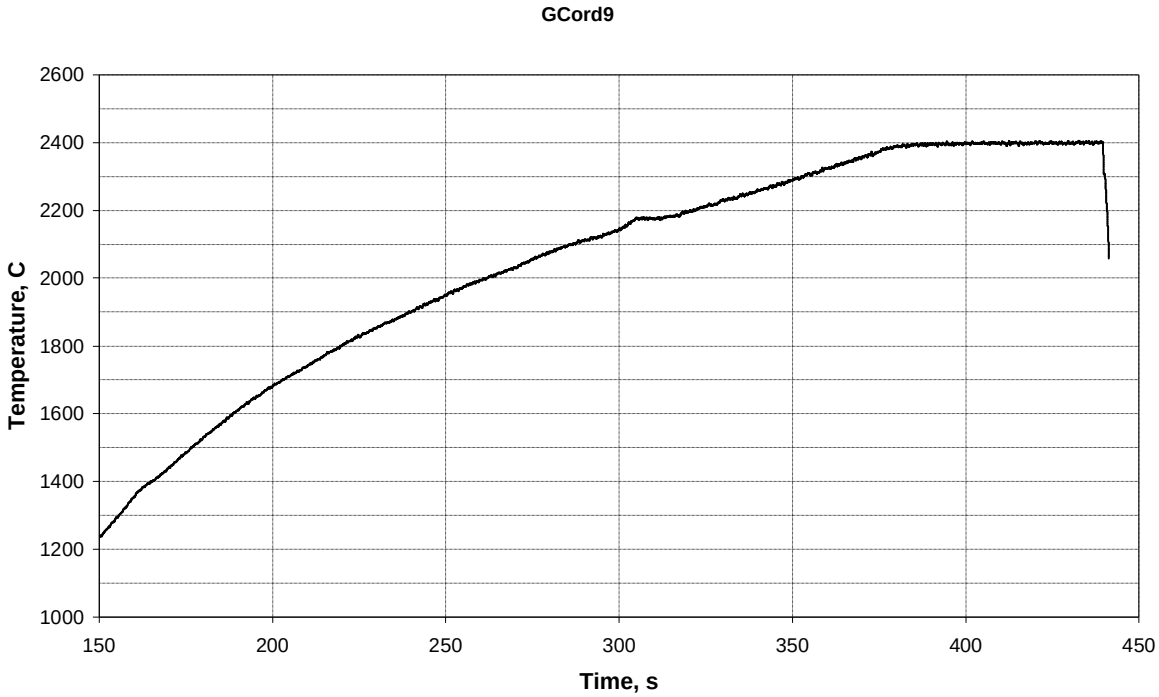

Fig. 10. Thermogram from GCord9

2.3. SEM/EDX results for the specimens in the UO_2–SiO_2 system

GCORD1

Longitudinal section of the crucible with specimen is given in Fig. 11. It shows melt segregation into two liquids, the upper one with numerous pores, and the bottom liquid.

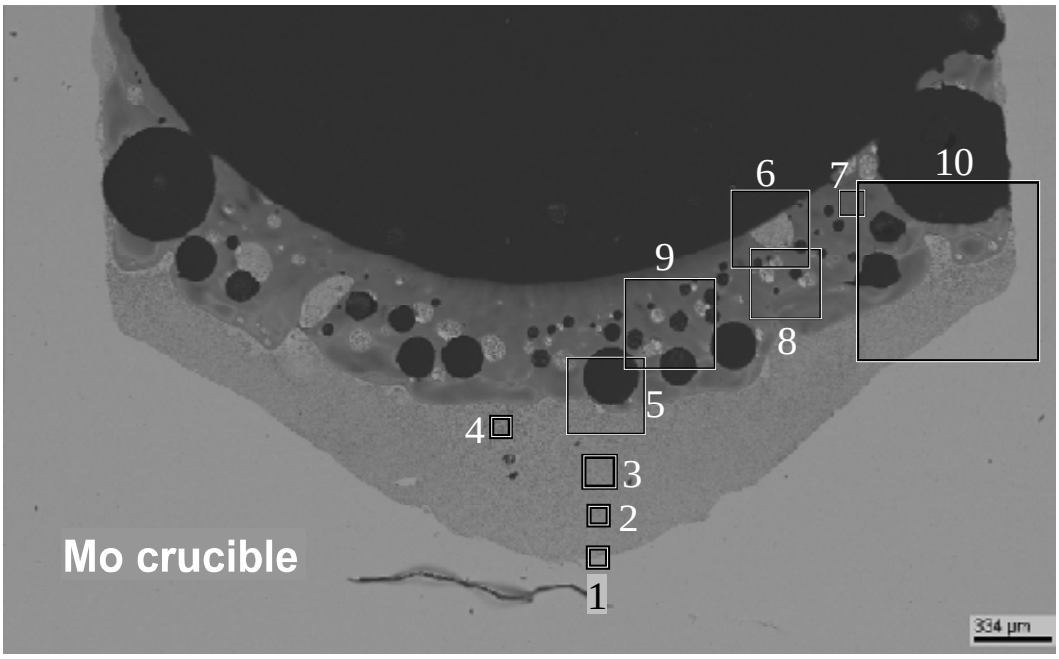

Fig. 11. SEM image of the longitudinal section with regions marked for SEM/EDX analysis in GCord1 (2140°C)

SEM/EDX results for the specimen are presented in Figs. 12-18 and in Tabs. 4-10.

Regions 1-4 correspond to the bottom liquid and are shown in Figs. 12-14.

Fig. 12, in its turn, demonstrates the bottom part of the quenched melt adjacent to the crucible.

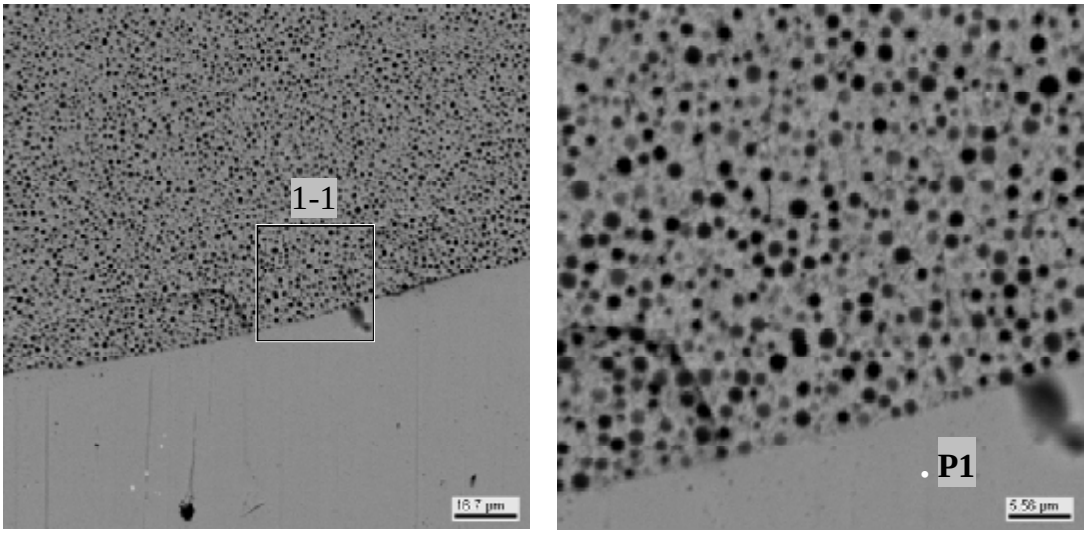

1 1-1

Fig. 12. Micrographs of region 1 in GCord1

Table 4. Data on region 1 EDX analysis

No.	U	Si	Mo
P1	100 % Mo		

The analysis results suggest that there was no interaction between the crucible and melt.

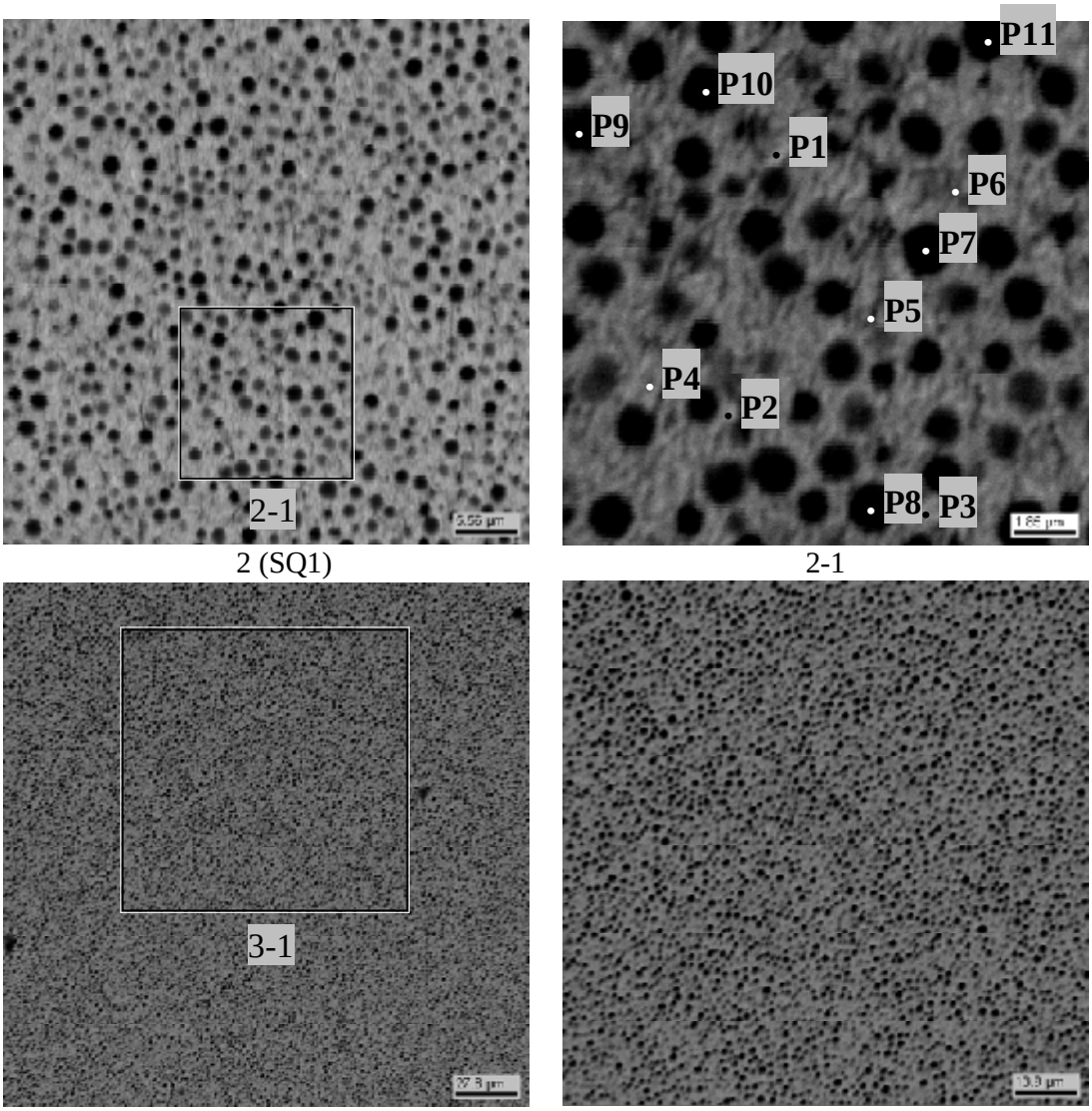

2 (SQ1) 2-1

3 (SQ2) 3-1 (SQ3)

Fig. 13. Micrographs of regions 2 & 3 from the bottom liquid in GCord1

Tab. 5 presents the EDX data for regions 2 and 3 in the squares (SQ1, SQ2 и SQ3) and points (P1-11).

Table 5. Data on regions 2 & 3 EDX analysis

No.		UO_2	SiO_2
SQ1	mass %	66.23	33.76
	mol.%	30.39	69.61
SQ2	mass %	64.49	35.5
	mol.%	28.79	71.21
SQ3	mass %	64.52	35.48
	mol.%	28.8	71.2
P1	mass %	71.97	28.02
	mol.%	36.37	63.63
P2	mass %	70.27	29.71
	mol.%	34.48	65.52
P3	mass %	71.05	28.94
	mol.%	35.33	64.67
P4	mass %	70.51	29.48
	mol.%	34.73	65.27
P5	mass %	68.02	31.97
	mol.%	32.13	67.87
P6	mass %	71.59	28.4
	mol.%	35.93	64.07
P7	mass %	54.13	45.86
	mol.%	20.8	79.2
P8	mass %	59.83	40.15
	mol.%	24.9	75.1
P9	mass %	58.37	41.62
	mol.%	23.79	76.21
P10	mass %	52.91	47.07
	mol.%	20	80
P11	mass %	53.35	46.63
	mol.%	20.29	79.71

The above results lead to a conclusion that the lighter-coloured ‘matrix’ phase in the lower layer is a liquid with a higher content of UO_2 (points P1 and P3). The rounded dark-coloured phase and the extended stripes represent the liquid with a higher content of SiO_2 (points P7-P11).

Micrographs in Fig. 14 were made with a large magnification and give an idea of the lower layer crystallization character.

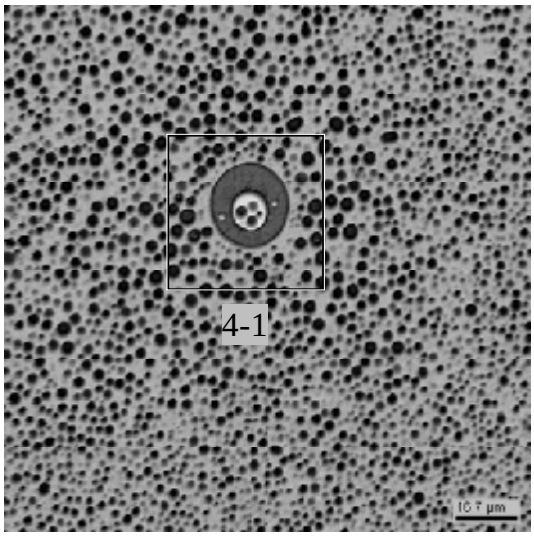

4

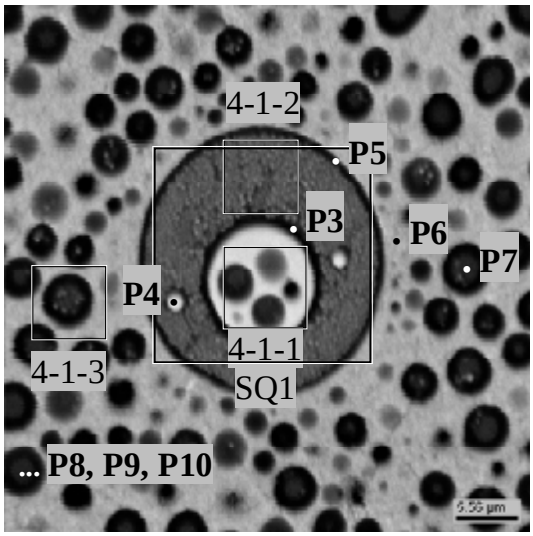

4-1

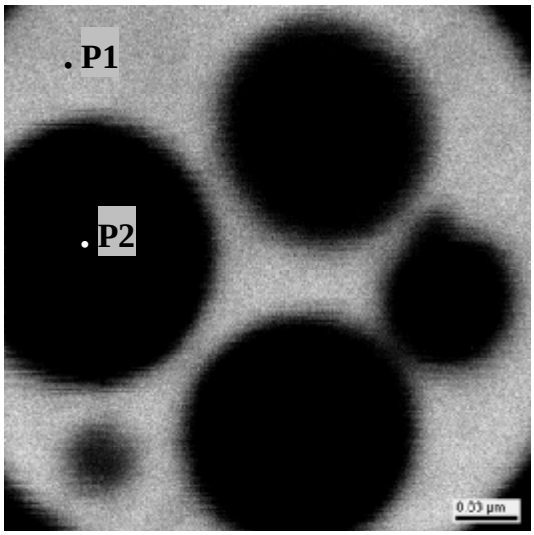

4-1-1 (SQ2)

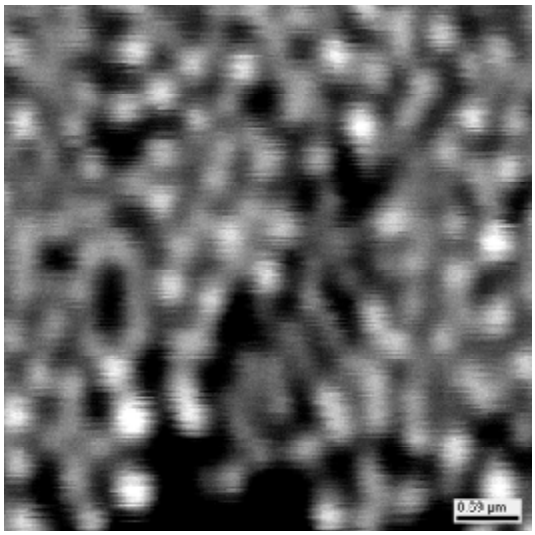

4-1-2 (SQ3)

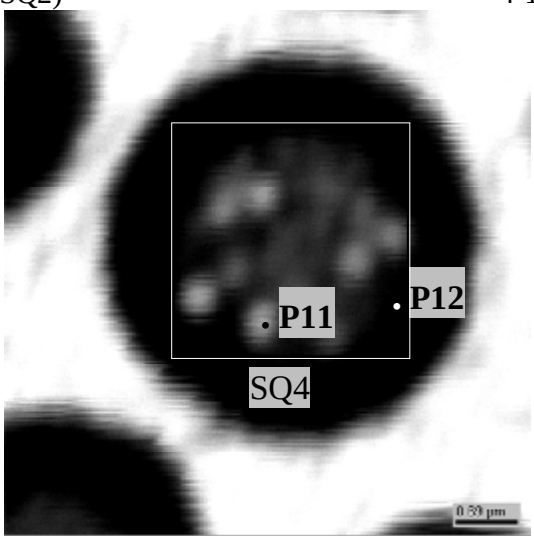

4-1-3

Fig. 14. Micrographs of region 4 from the bottom layer in GCord1

Table 6. Data on region 4 EDX analysis

No.		UO_2	SiO_2
SQ1	mass %	51.94	48.06
	mol.%	19.39	80.61
SQ2	mass %	58.25	41.75
	mol.%	23.69	76.31
SQ3	mass %	42.11	57.89
	mol.%	13.93	86.07
SQ4	mass %	36.86	63.14
	mol.%	11.5	88.5
P1	mass %	82.55	17.45
	mol.%	51.28	48.72
P2	mass %	43.89	56.11
	mol.%	14.83	85.17
P3	mass %	36.81	63.19
	mol.%	11.47	88.53
P4	mass %	64.55	35.45
	mol.%	28.83	71.17
P5	mass %	39.1	60.9
	mol.%	12.5	87.5
P6	mass %	73.11	26.89
	mol.%	37.69	62.31
P7	mass %	29.81	70.19
	mol.%	8.63	91.37
P8	mass %	28.04	71.96
	mol.%	7.98	92.02
P9	mass %	30.23	69.76
	mol.%	8.79	91.21
P10	mass %	31.02	68.98
	mol.%	9.1	90.9
P11	mass %	37.61	62.39
	mol.%	11.83	88.17
P12	mass %	36.85	63.15
	mol.%	11.49	88.51

The lighter-coloured ‘matrix’ phase with a higher content of UO_2 is also observed here (points P1, P6, P11). The rounded phase of darker colour contains more of SiO_2 (e.g., points P2, P7).

Fig. 15 shows the boundary region between two liquids. The findings for this region are presented in Tab. 7.

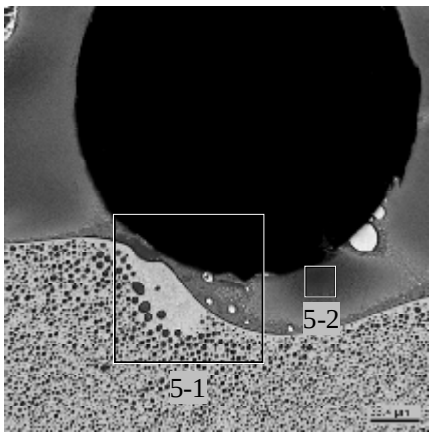

5

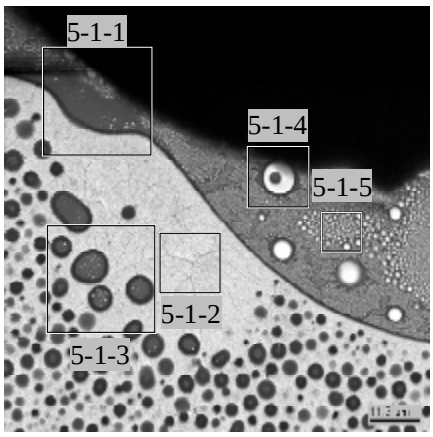

5-1

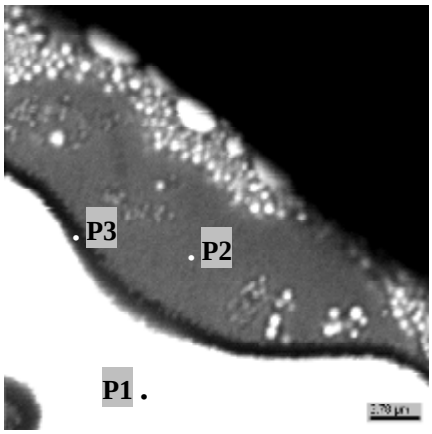

5-1-1

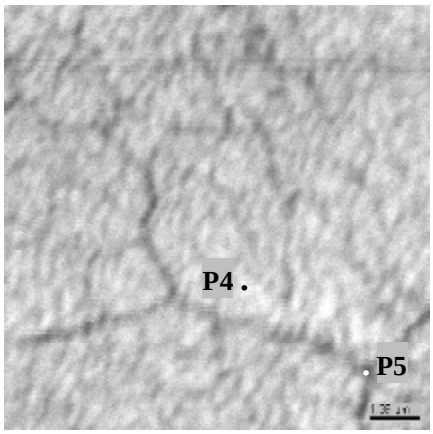

5-1-2 (SQ1)

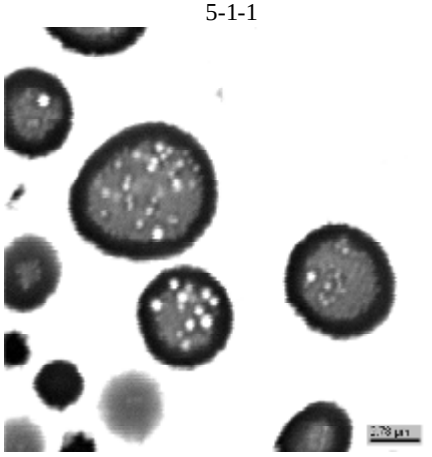

5-1-3

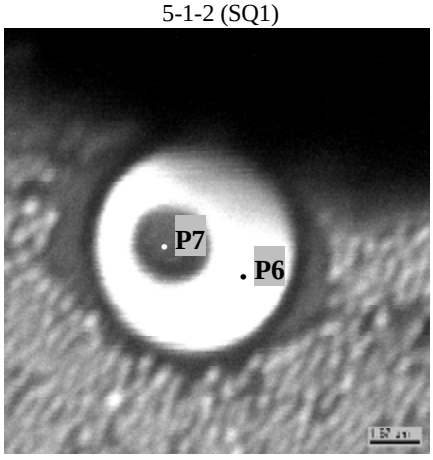

5-1-4

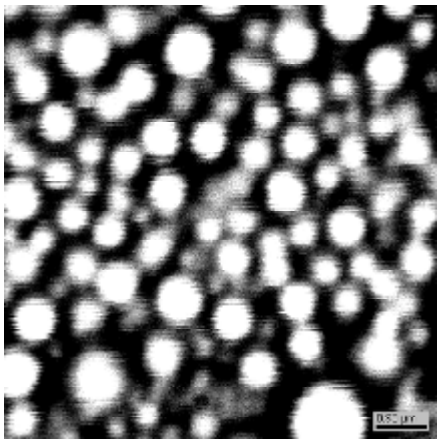

5-1-5 (SQ2)

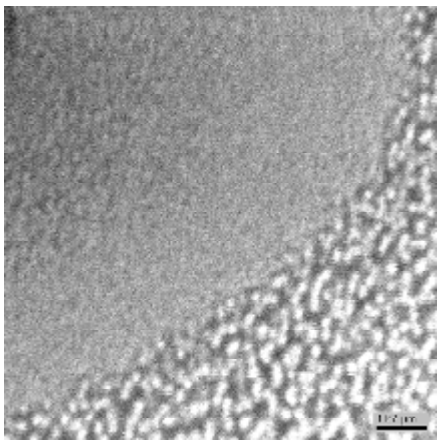

5-2 (SQ3)

Fig. 15. Micrographs of region 5 in GCord1

Table 7. Data on region 5 EDX analysis

No.		UO_2	SiO_2
SQ1	mass %	74.7	25.3
	mol.%	39.65	60.35
SQ2	mass %	47.2	52.8
	mol.%	16.59	83.41
SQ3	mass %	22.75	77.25
	mol.%	6.15	93.85
P1	mass %	67.56	32.44
	mol.%	31.67	68.33
P2	mass %	22.22	77.78
	mol.%	5.98	94.02
P3	mass %	32.84	67.16
	mol.%	9.81	90.19
P4	mass %	76.76	23.24
	mol.%	42.36	57.64
P5	mass %	72.04	27.96
	mol.%	36.44	63.56
P6	mass %	83.73	16.27
	mol.%	53.38	46.62
P7	mass %	48.34	51.66
	mol.%	17.24	82.76

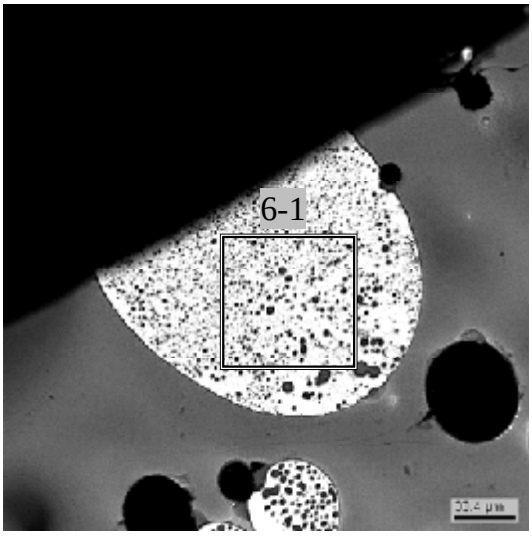

6

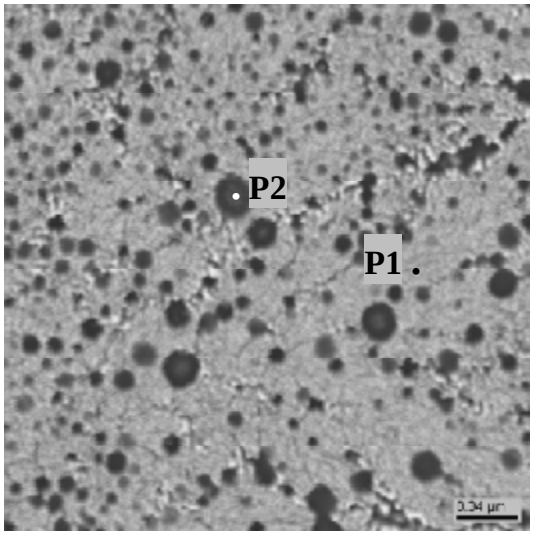

6-1 (SQ1)

Fig. 16. Micrographs of region 6 from the upper layer in GCord1

Table 8. Data on region 6 EDX analysis

No.		UO_2	SiO_2
SQ1	mass %	64.83	35.16
	mol.%	29.09	70.91
P1	mass %	76.58	23.42
	mol.%	42.12	57.88
P2	mass %	34.96	65.02
	mol.%	10.68	89.32

It is desirable to stress similarity between composition of the marked rounded formation in the upper liquid and that of the bottom layer (Tab. 8, SQ1 and Tab. 5, SQ1 and SQ2). A possible reason is that the time of exposure (3 sec) was insufficient for the completion of melt stratification into two layers, and fragments of the bottom liquid, poorer in SiO_2, remained in the upper, denser one (Tab. 7, points P1 and P2 corresponding to compositions of the bottom and upper liquids, respectively).

A similar picture of the incomplete stratification of the upper layer can be also seen in Figs. 17, 18. A possible reason may be the insufficient exposure at a high melt density.

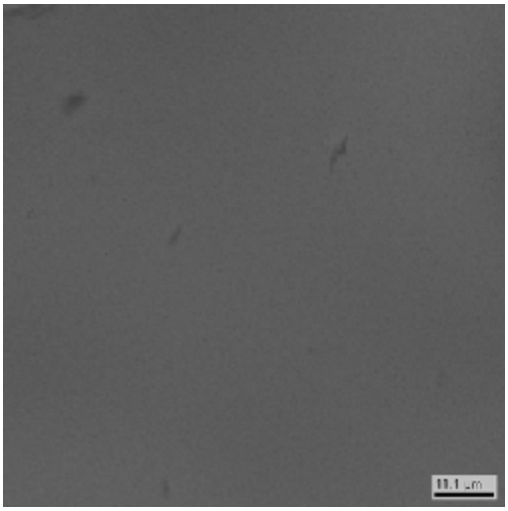

7 (SQ1)

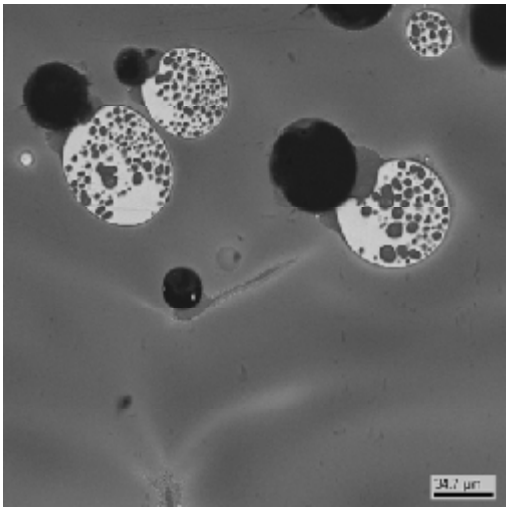

8 (SQ2)

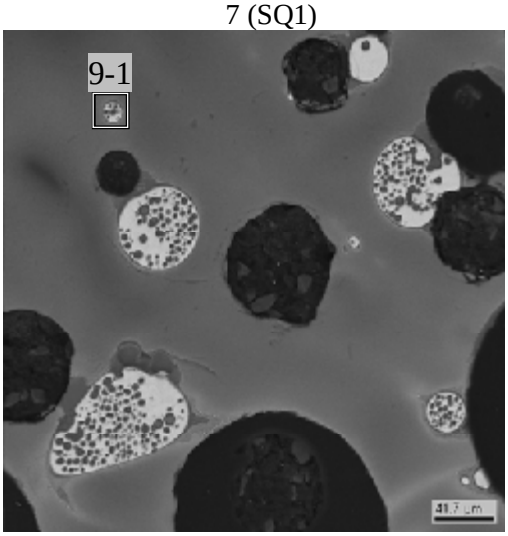

9 (SQ3)

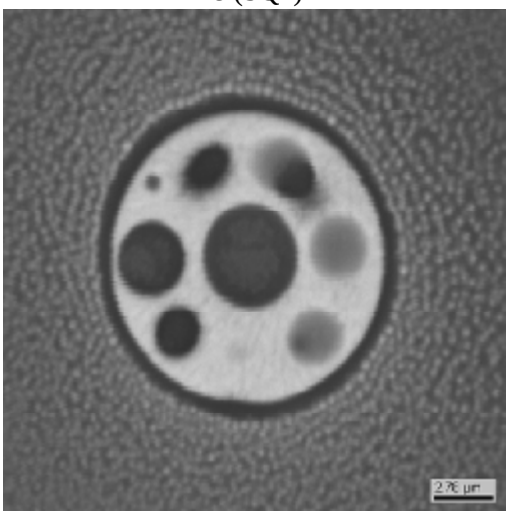

9-1

Fig. 17. Micrographs of regions 7-9 from the upper layer in GCord1

Table 9. Data on regions 7-9 EDX analysis

No.		UO_2	SiO_2
SQ1	mass %	25.91	74.09
	mol.%	7.22	92.78
SQ2	mass %	33.27	66.73
	mol.%	9.98	90.02
SQ3	mass %	29.43	70.57
	mol.%	8.49	91.51

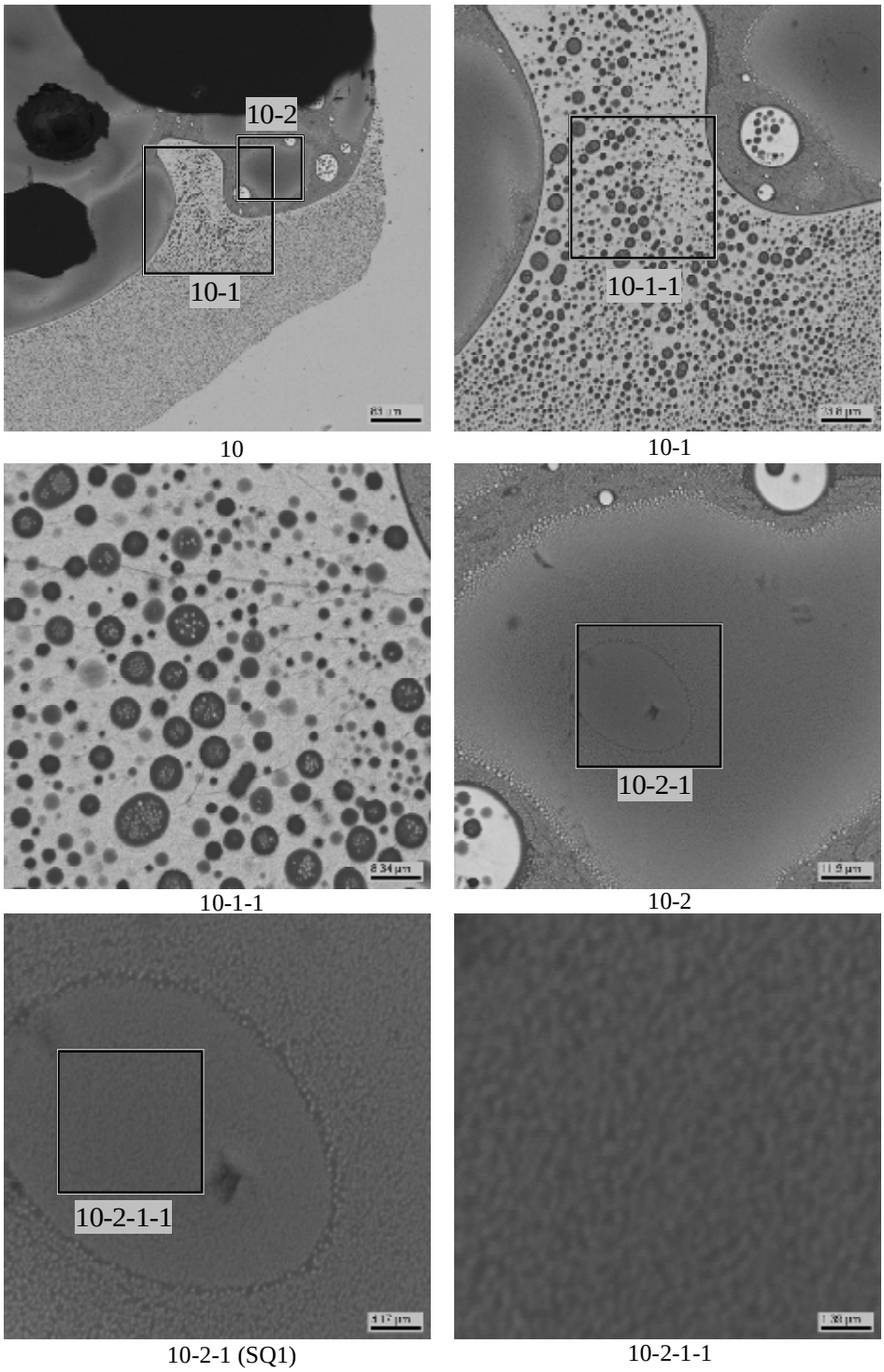

10 | 10-1
10-1-1 | 10-2
10-2-1 (SQ1) | 10-2-1-1

Fig. 18. Micrographs of region 10 in GCord1

Table 10. Data on region 10 EDX analysis

No.		UO_2	SiO_2
SQ1	mass %	22.02	77.98
	mol.%	5.91	94.09

GCord2

Fig. 19 offers a SEM image of the longitudinal section of the crucible with specimen subjected to thermal treatment at 2000°C with subsequent quenching.

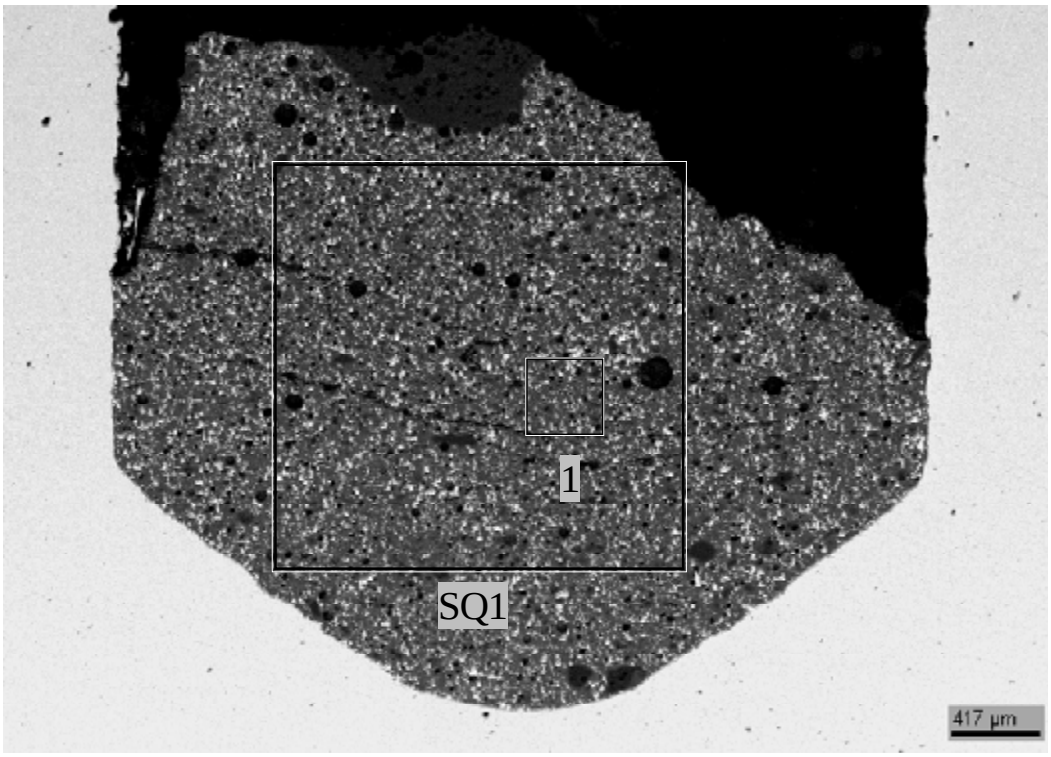

Fig. 19. SEM image of the crucible longitudinal section in GCord2 with regions marked for SEM/EDX analysis (2000°C)

It can be seen from the figure that melting of the specimen at this temperature was incomplete. Fig. 20 and Tab. 11 contain the results of analysis of a smaller region, as well as data on individual phases (P1, P2).

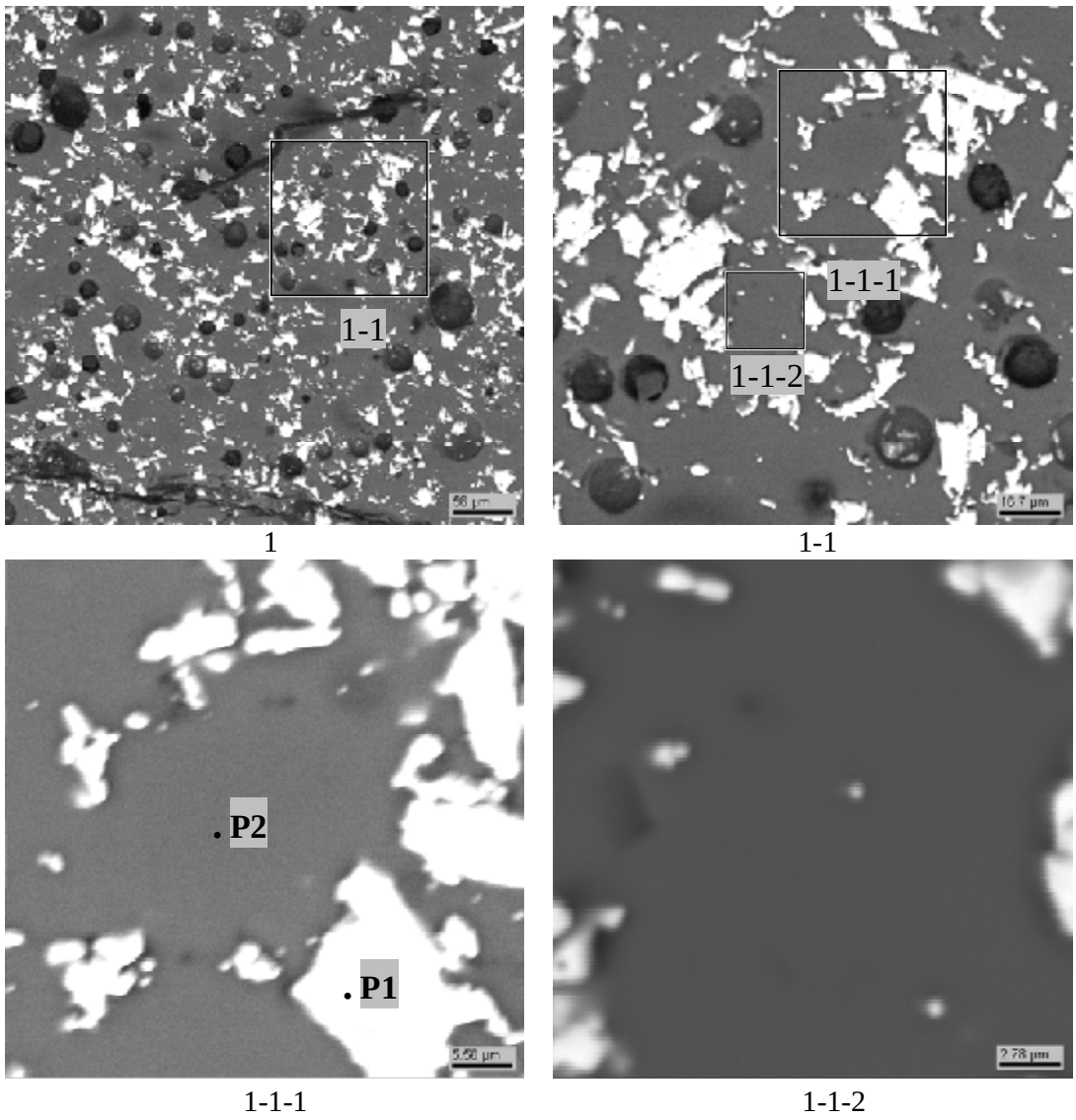

1 1-1

1-1-1 1-1-2

Fig. 20. Micrographs of region 1 in GCord2

Table 12. Data on region 1 EDX analysis

No.		UO_2	SiO_2
P1	mass %	98.05	1.95
	mol.%	91.78	8.22
P2	mass %	15.00	85.00
	mol.%	3.78	96.22

It may be seen from Fig. 20 and data in Tab. 11 that the specimen consists of two phases: a phase strongly enriched in UO_2, and another one, strongly enriched in SiO_2, respectively.

GCord5

Fig. 21 offers a SEM image of the longitudinal section of the molybdenum crucible with specimen subjected to thermal treatment at 2080°C with subsequent quenching.

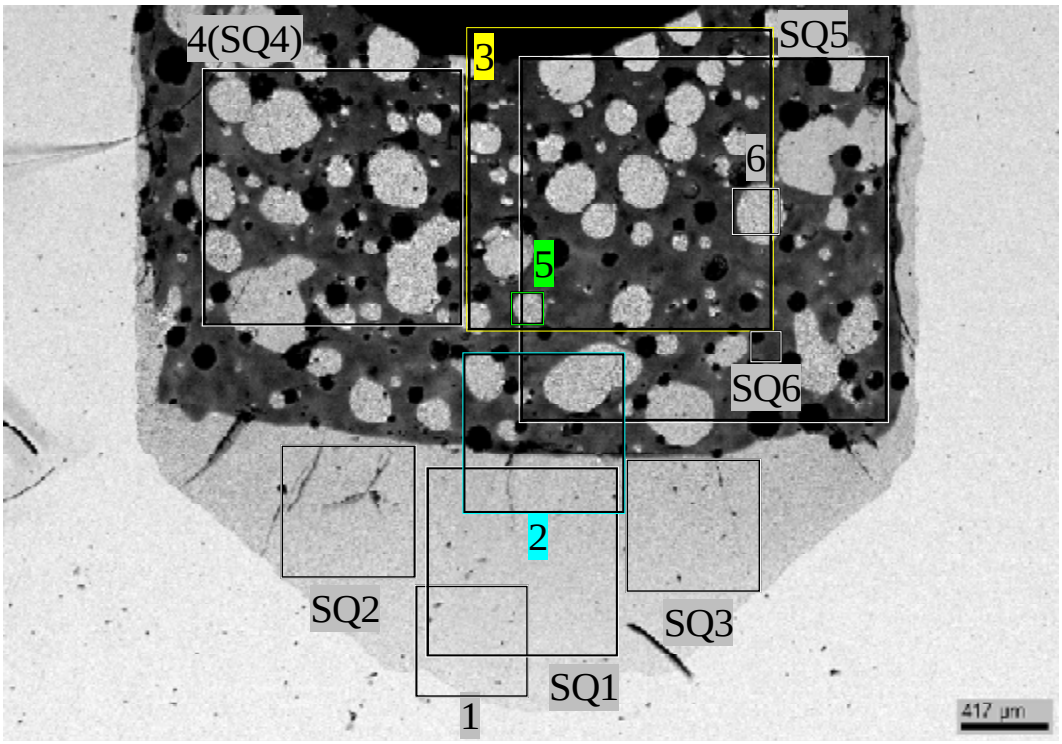

Fig. 21. SEM image for the longitudinal section of crucible in GCord5 with regions marked for SEM/EDX analysis (2080°C)

The figure demonstrates the presence of stratification into two layers, the upper and bottom ones. The upper layer features numerous large pores and rounded inclusions. Phase contrast shows them to be close to the bottom layer.

Tab. 12 contains the results of analysis of different regions of the section in question – of both the bottom layer (SQ1, SQ2, SQ3) enriched in UO_2, and the upper one (SQ4, SQ5, SQ6) enriched in SiO_2.

Table 12. EDX data for the areas of the crucible longitudinal section in GCord5

No.		UO_2	SiO_2
SQ1	mass %	67.66	32.34
	mol.%	31.76	68.24
SQ2	mass %	68.33	31.67
	mol.%	32.44	67.56
SQ3	mass %	67.46	32.54
	mol.%	31.57	68.43
SQ4	mass %	43.57	56.43
	mol.%	14.66	85.34
SQ5	mass %	43.04	56.96
	mol.%	14.40	85.60
SQ6	mass %	27.92	72.08
	mol.%	7.94	92.06

The bottom layer consists of two phases: a light-coloured ‘matrix’ phase with a higher content of UO_2, and a dark-coloured, rounded phase with a higher content of SiO_2.

The liquid bottom layer and boundary region shown in Figs. 22 and 23 are very typical for this specimen. Table 13 presents the results of squares analysis.

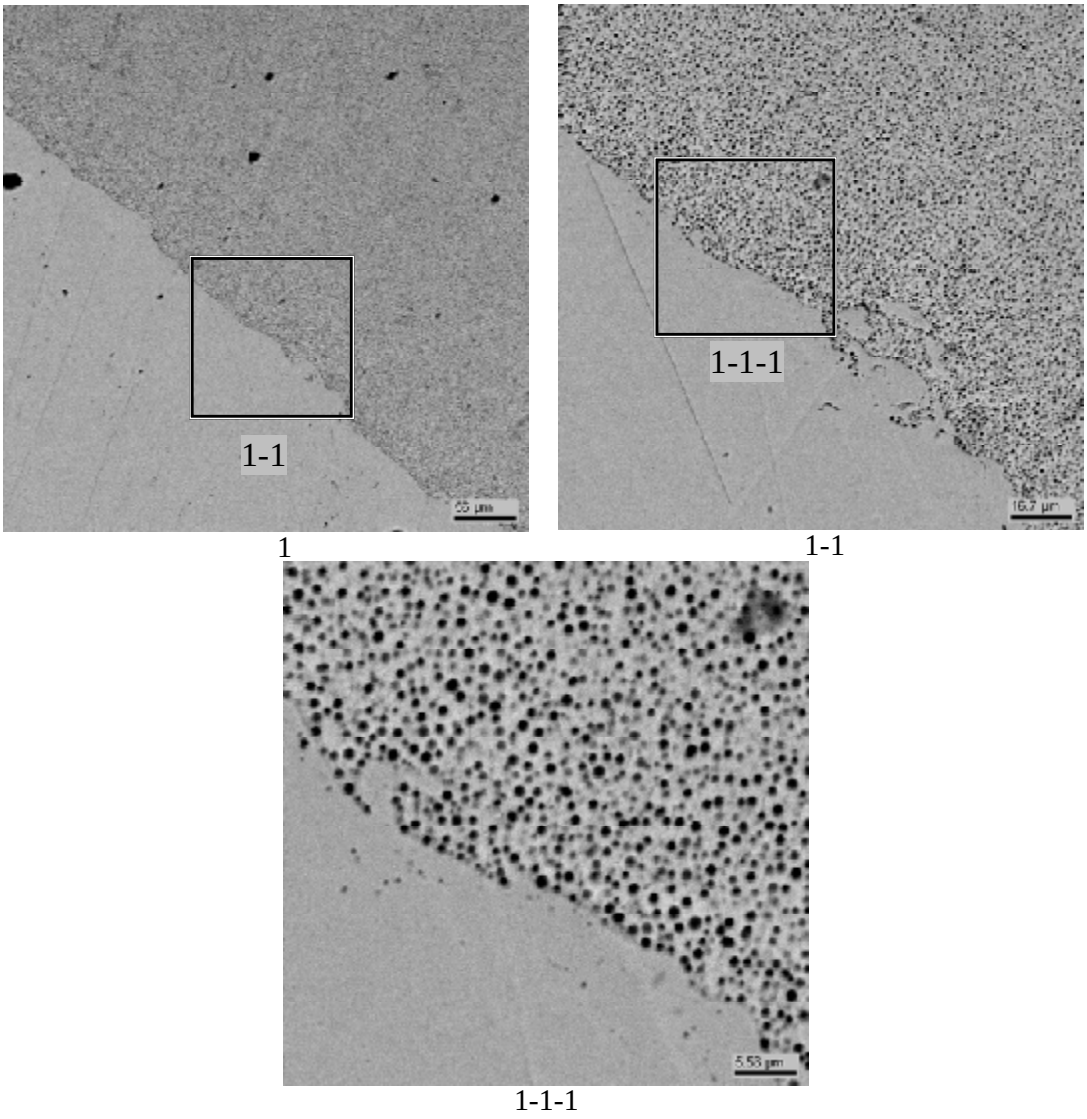

1 1-1 1-1-1

Fig. 22. Micrographs of region 1 from the bottom layer in GCord5

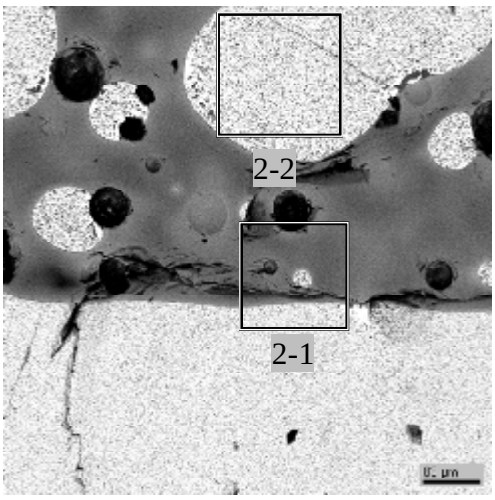

2

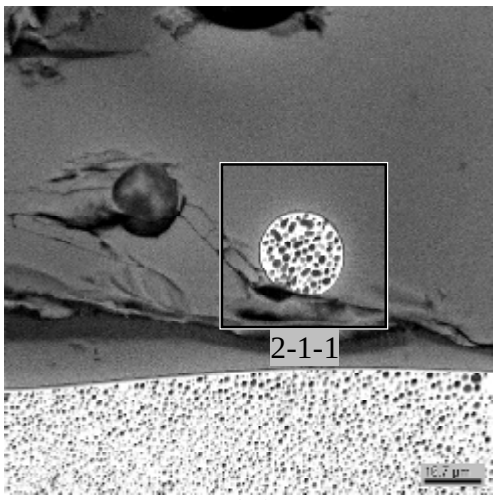

2-1

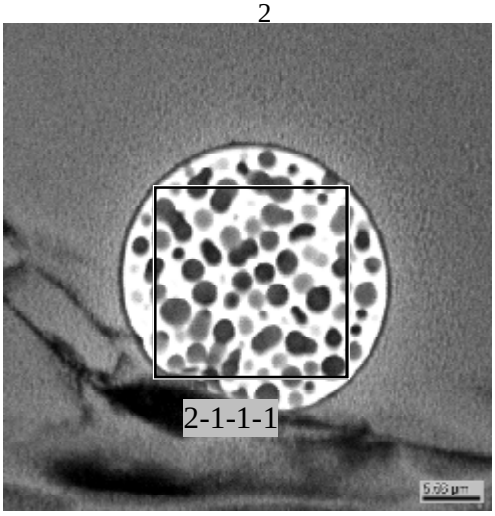

2-1-1

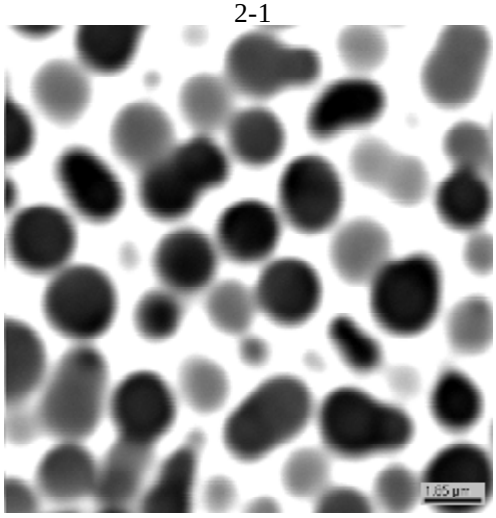

2-1-1-1(SQ1)

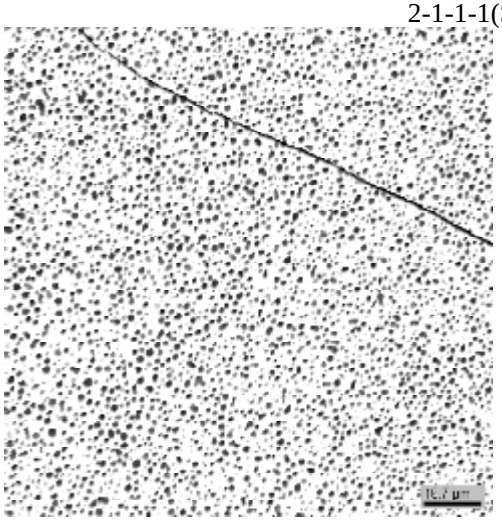

2-2(SQ2)

Fig. 23. Micrographs of the boundary region 2 in GCord5

Table 13. Data on region 2 EDX analysis

No.		UO_2	SiO_2
SQ1	mass %	58.60	41.40
	mol.%	23.95	76.05
SQ2	mass %	65.32	34.68
	mol.%	29.53	70.47

Figs. 24-26 present a very typical for this test appearance of the stratified melt upper layer. In this case, like in GCord1, a large number of light-coloured rounded formations is observed. Compositions of the investigated regions are given in Tabs. 14 and 15.

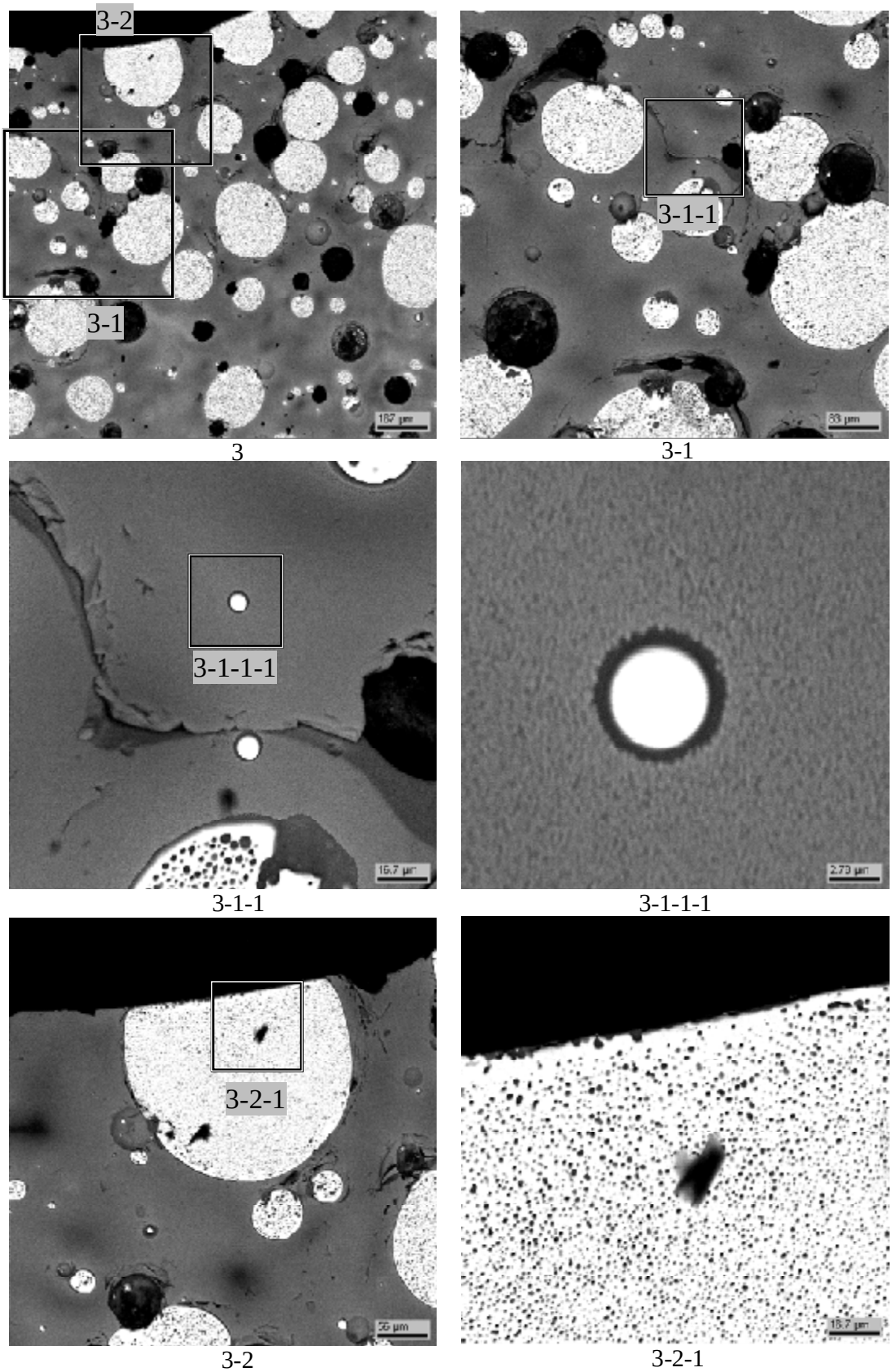

Fig. 24. Micrographs of region 3 from the upper layer in GCord5

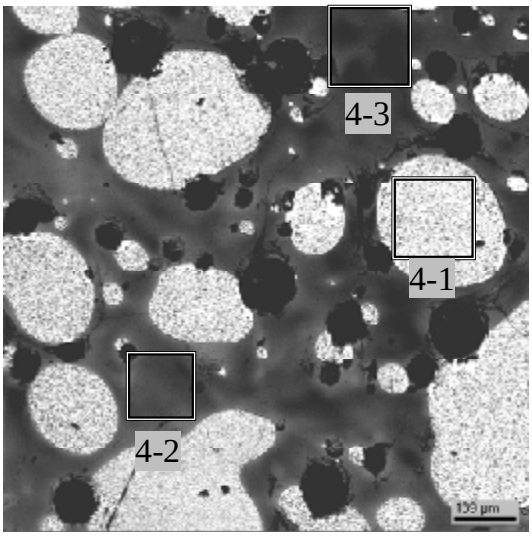

4

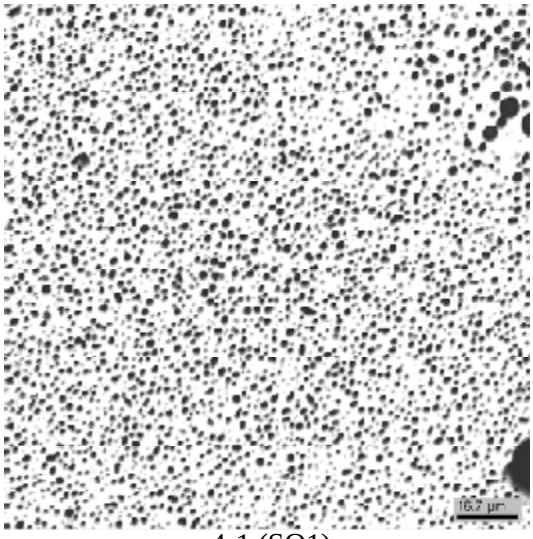

4-1 (SQ1)

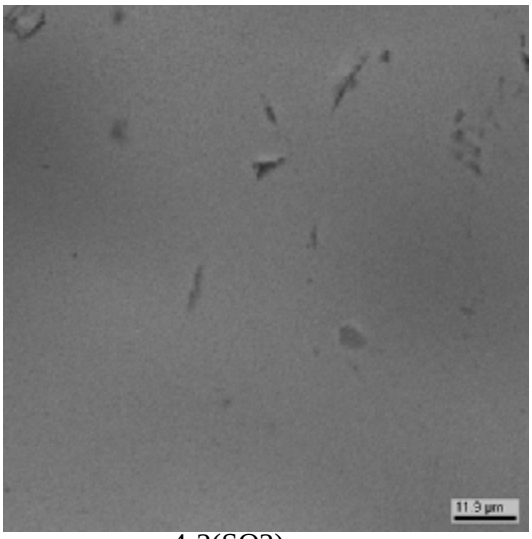

4-2(SQ2)

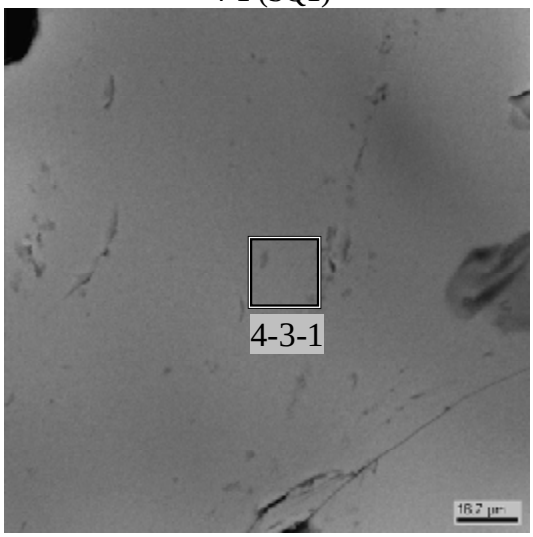

4-3(SQ3)

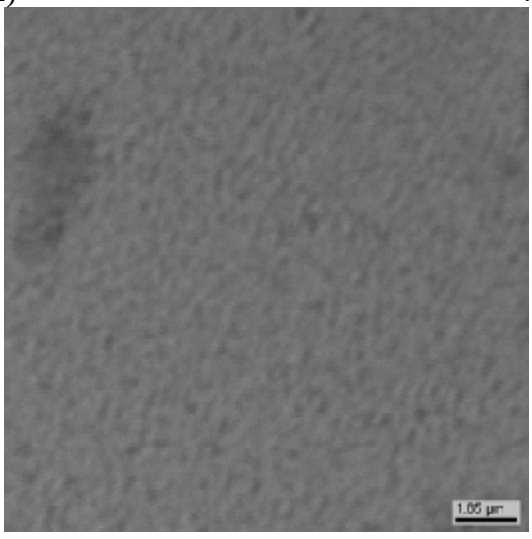

4-3-1(SQ4)

Fig. 25. Micrographs of region 4 from the upper layer in GCord5

Table 14. Data on region 4 EDX analysis

No.		UO_2	SiO_2
SQ1	mass %	43.57	56.43
	mol.%	14.66	85.34
SQ2	mass %	28.64	71.36
	mol.%	8.20	91.80
SQ3	mass %	31.11	68.89
	mol.%	9.13	90.87
SQ4	mass %	28.97	71.03
	mol.%	8.32	91.68

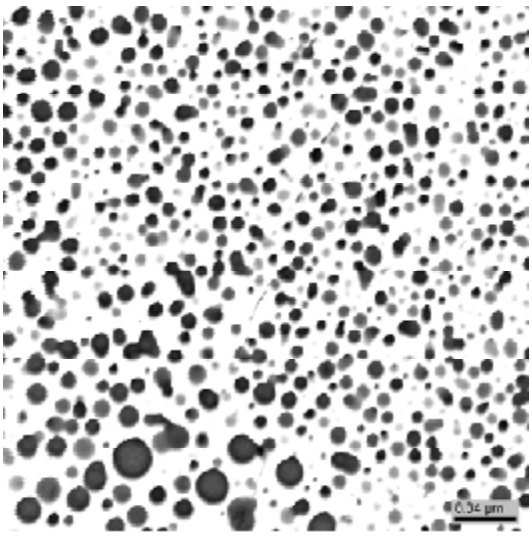

5 (SQ1)

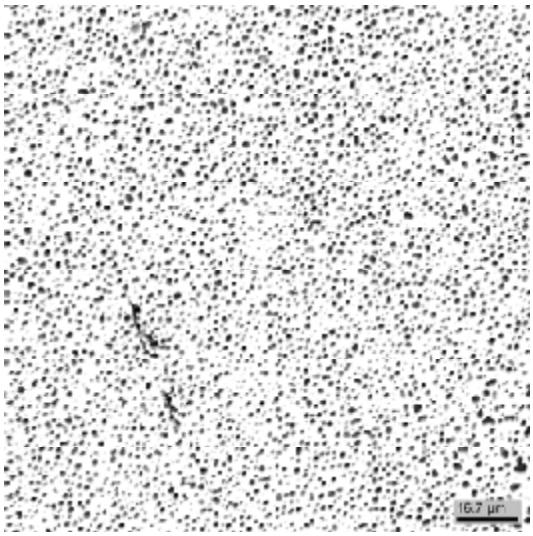

6 (SQ2)

Fig. 26. Micrographs of regions 5 & 6 with rounded formations from the upper layer in GCord5

Table 15. Data on regions 5 & 6 EDX analysis

No.		UO_2	SiO_2
SQ1	mass %	63.46	36.54
	mol.%	27.87	72.13
SQ2	mass %	65.56	34.44
	mol.%	29.76	70.24

In general, the upper liquid is richer in SiO_2 in comparison with the bottom one. The large number of rounded formations close in their composition to the bottom liquid (compare Tab. 13, SQ1 and SQ3, and Tab. 16, SQ1 and SQ2) is obviously due to the insufficient melt exposure. A possible reason is the high density of the upper liquid (with a large percentage of SiO_2) which did not let the UO_2-rich liquid to descend to the crucible bottom.

GCord3

Fig. 27 offers a SEM image of the longitudinal section of the molybdenum crucible with specimen subjected to thermal treatment at 2140°C with subsequent quenching.

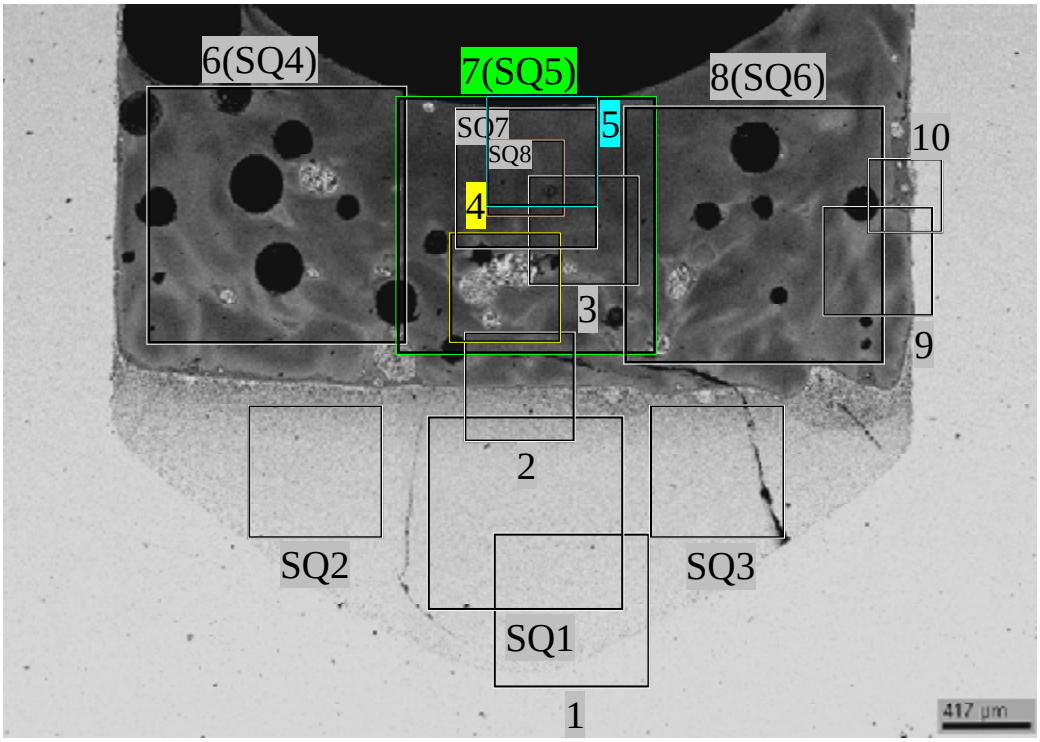

Fig. 27. SEM image of the longitudinal section of the crucible in GCord3 with regions marked for SEM/EDX analysis (2140°C)

The figure shows that the melt stratifies into two layers: the upper and lower ones. The upper layer features a large number of big pores.

Tab. 16 contains the results of analysis of different regions of the section in question, from both the bottom layer (SQ1-SQ3) enriched in UO_2, and the upper one (SQ4-SQ8) enriched in SiO_2.

Table 16. EDX data for the longitudinal section of the crucible in the areas marked in Fig. 30

No.		UO_2	SiO_2
SQ1	mass %	71.25	28.75
	mol.%	35.55	64.45
SQ2	mass %	71.81	28.19
	mol.%	36.17	63.83
SQ3	mass %	71.96	28.04
	mol.%	36.34	63.66
SQ4	mass %	40.29	59.71
	mol.%	13.06	86.94
SQ5	mass %	34.04	65.96
	mol.%	10.3	89.7
SQ6	mass %	36.19	63.81
	mol.%	11.2	88.8
SQ7	mass %	28.25	71.75
	mol.%	8.05	91.95
SQ8	mass %	27.66	72.34
	mol.%	7.84	92.16

Figs. 28-35 show in succession fragments of the bottom liquid, boundary region, and the upper liquid, while Tabs. 18-20 offer the corresponding EDX data for both areas and points.

In contrast to GCORD5, a smaller number of rounded formations in both upper layer of the stratified melt and boundary region should be mentioned.

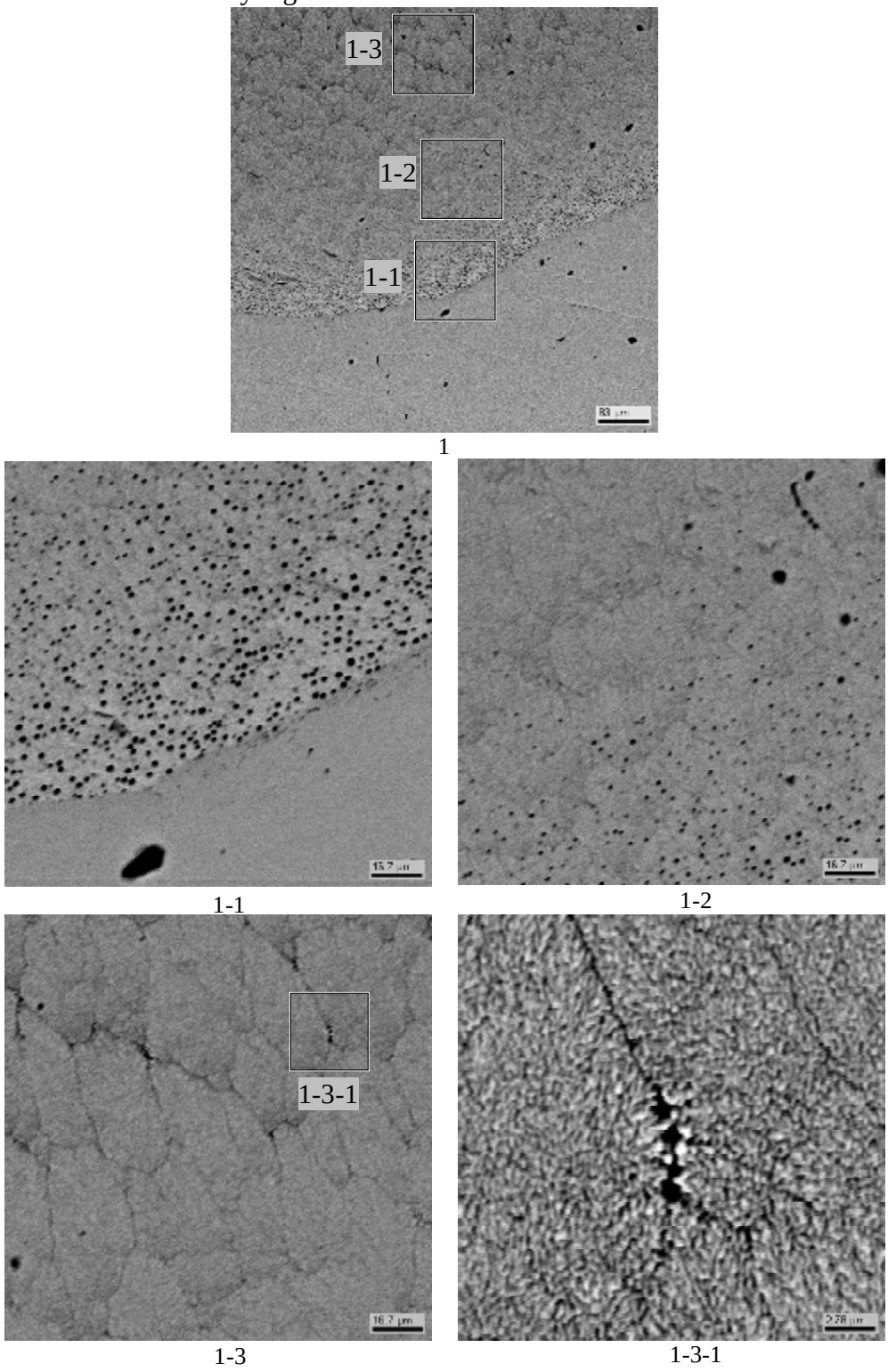

Fig. 28. Micrographs of region 1 from the bottom layer in Gcord3

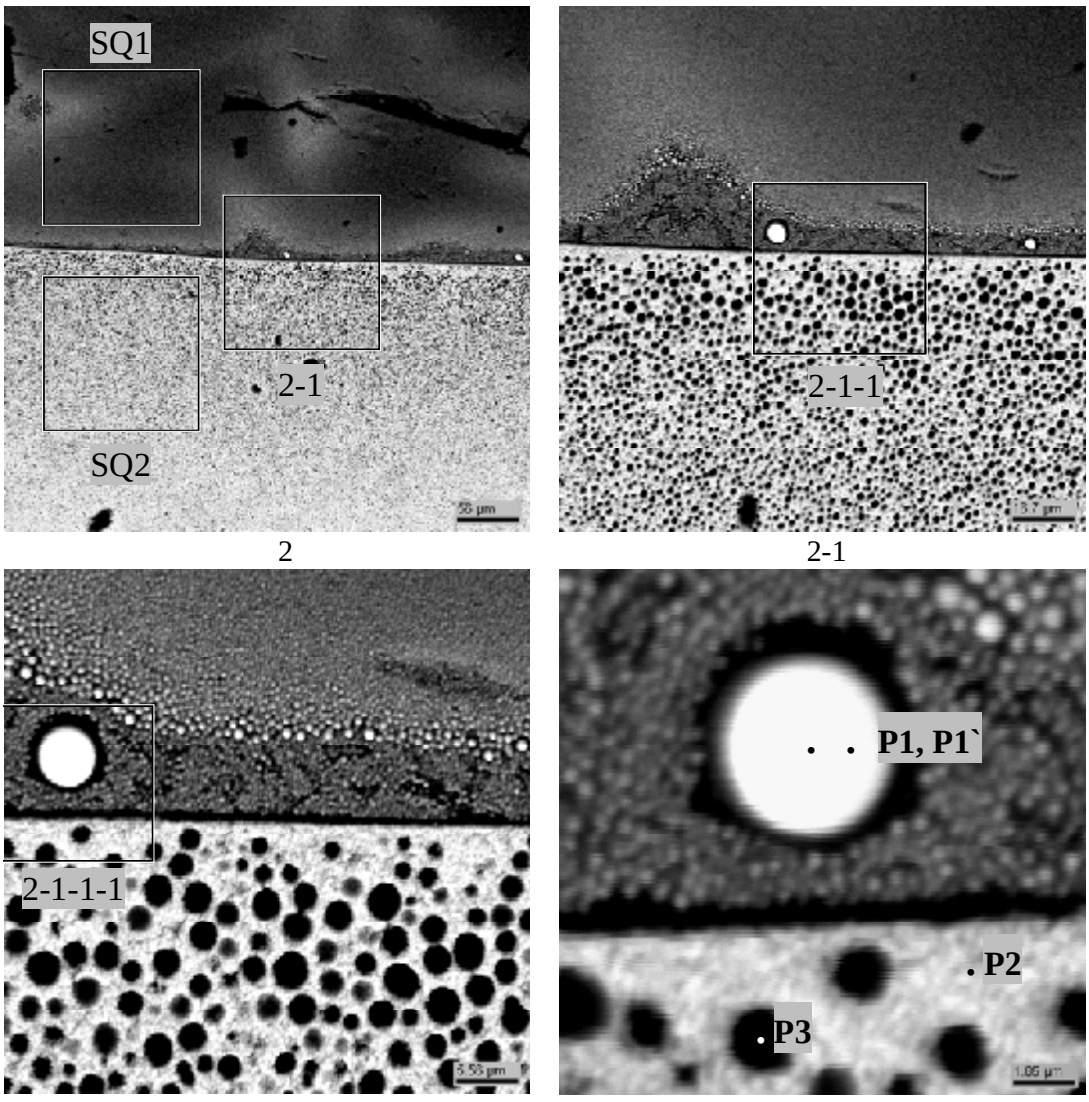

2 2-1

2-1-1 2-1-1-1

Fig. 29. Micrographs of fragment 2 from boundary region between the layers in Gcord3

Table 17. Data on region 2 EDX analysis

No.		UO_2	SiO_2
SQ1	mass %	37.20	62.80
	mol.%	11.64	88.36
SQ2	mass %	67.68	32.32
	mol.%	31.78	68.22
P1	mass %	84.17	15.83
	mol.%	54.20	45.80
P1`	mass %	81.73	18.27
	mol.%	49.89	50.11
P2	mass %	73.44	26.56
	mol.%	38.09	61.91
P3	mass %	33.94	66.06
	mol.%	10.26	89.74

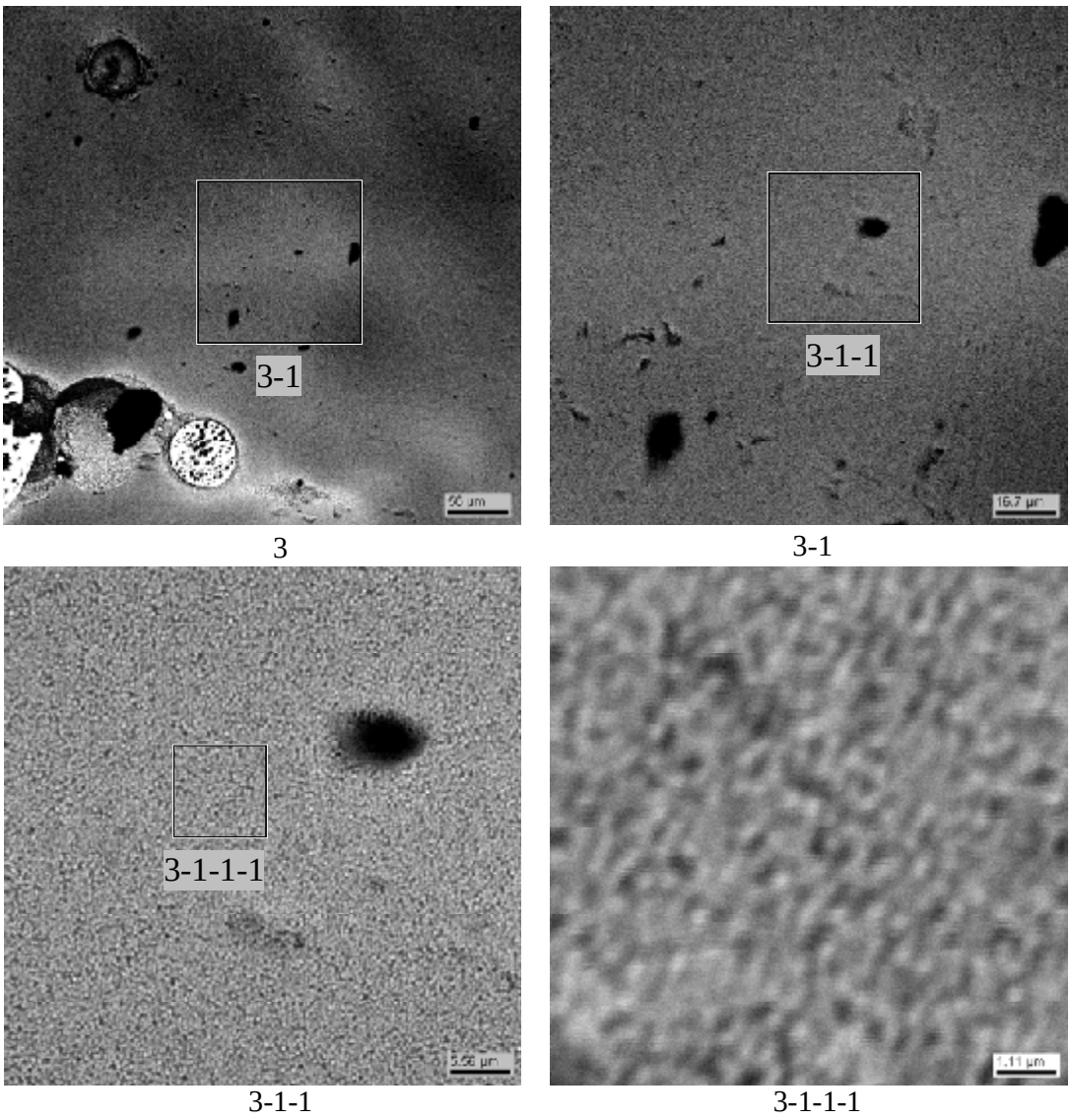

3 3-1

3-1-1 3-1-1-1

Fig. 30. Micrographs of region 3 from the upper layer in Gcord3

Some amount of light-coloured rounded formations can be observed in the upper layer (Fig. 31). Microstructurally, they are close to the bottom layer of the stratified melt, but their composition is different (Tab. 16, SQ1-SQ3 and Tab. 19, SQ1, SQ2). The said difference is presumably due to the failure to achieve equilibrium in the test.

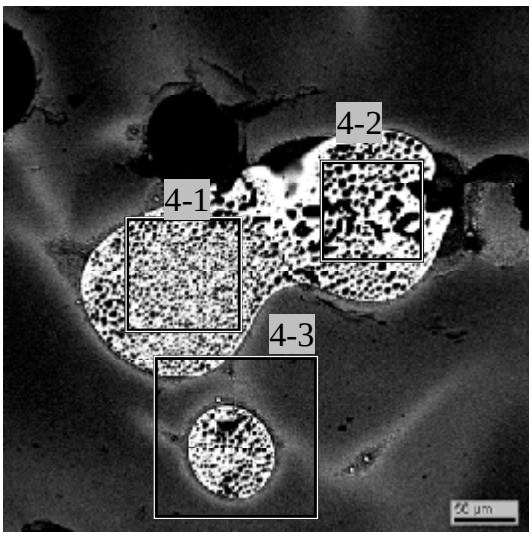

4

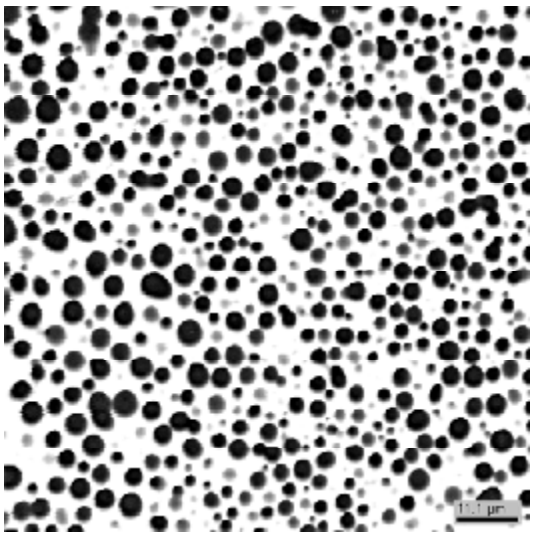

4-1 (SQ1)

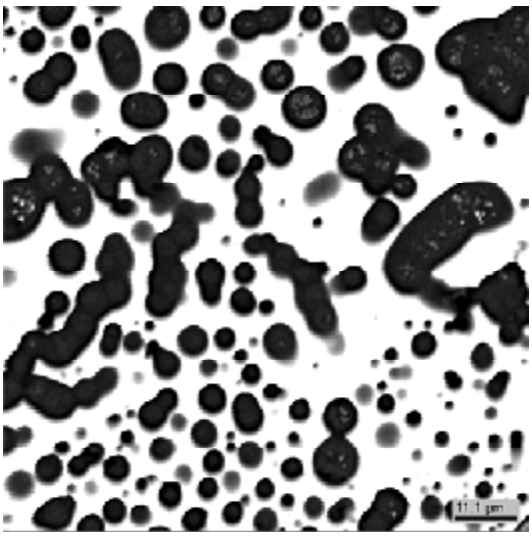

4-2 (SQ2)

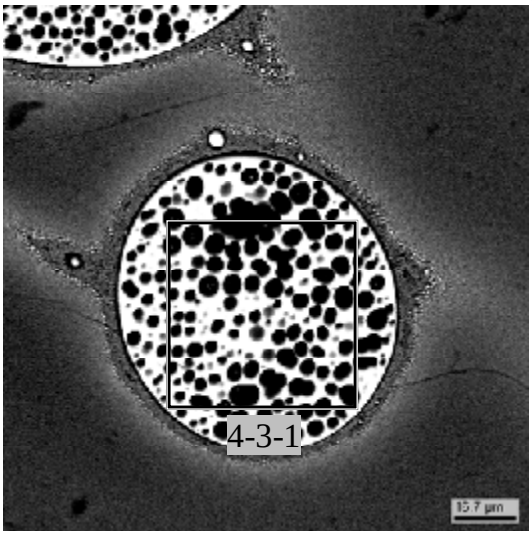

4-3

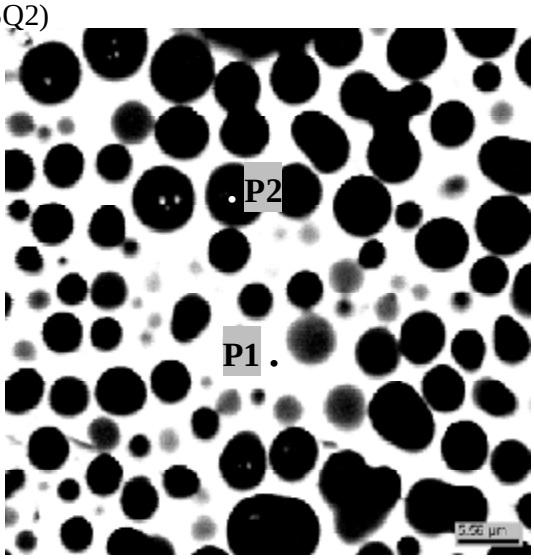

4-3-1 (SQ3)

Fig. 31. Micrographs of region 4 from the upper layer in Gcord3

Table 18. Data on region 4 EDX analysis

No.		UO_2	SiO_2
SQ1	mass %	55.93	44.07
	mol.%	22.02	77.98
SQ2	mass %	53.89	46.11
	mol.%	20.64	79.36
SQ3	mass %	54.43	45.57
	mol.%	20.99	79.01
P1	mass %	80.81	19.19
	mol.%	48.38	51.62
P2	mass %	18.99	81.01
	mol.%	4.96	95.04

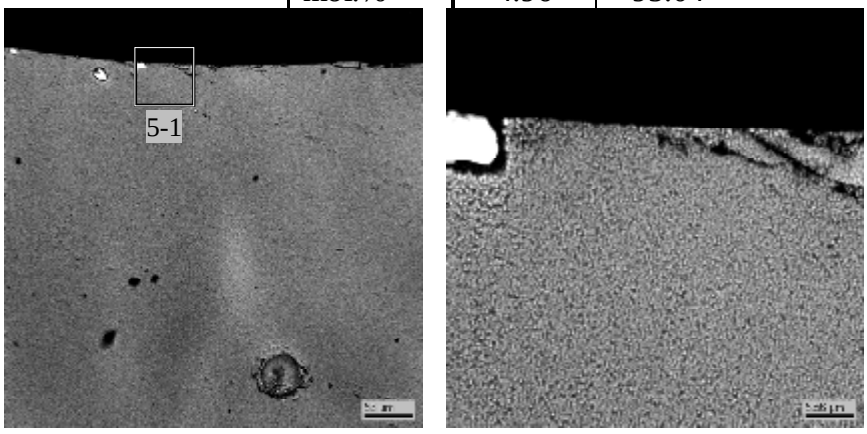

5 5-1

Fig. 32. Micrographs of region 5 from the upper layer in GCord3

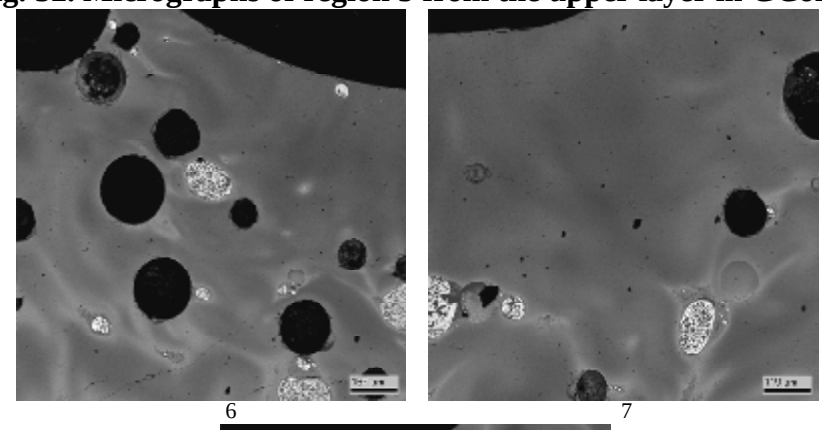

6 7

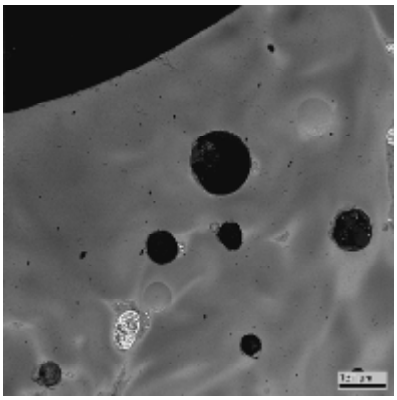

8

Fig. 33. Micrographs of regions 6, 7 & 8 from the upper layer in GCord3

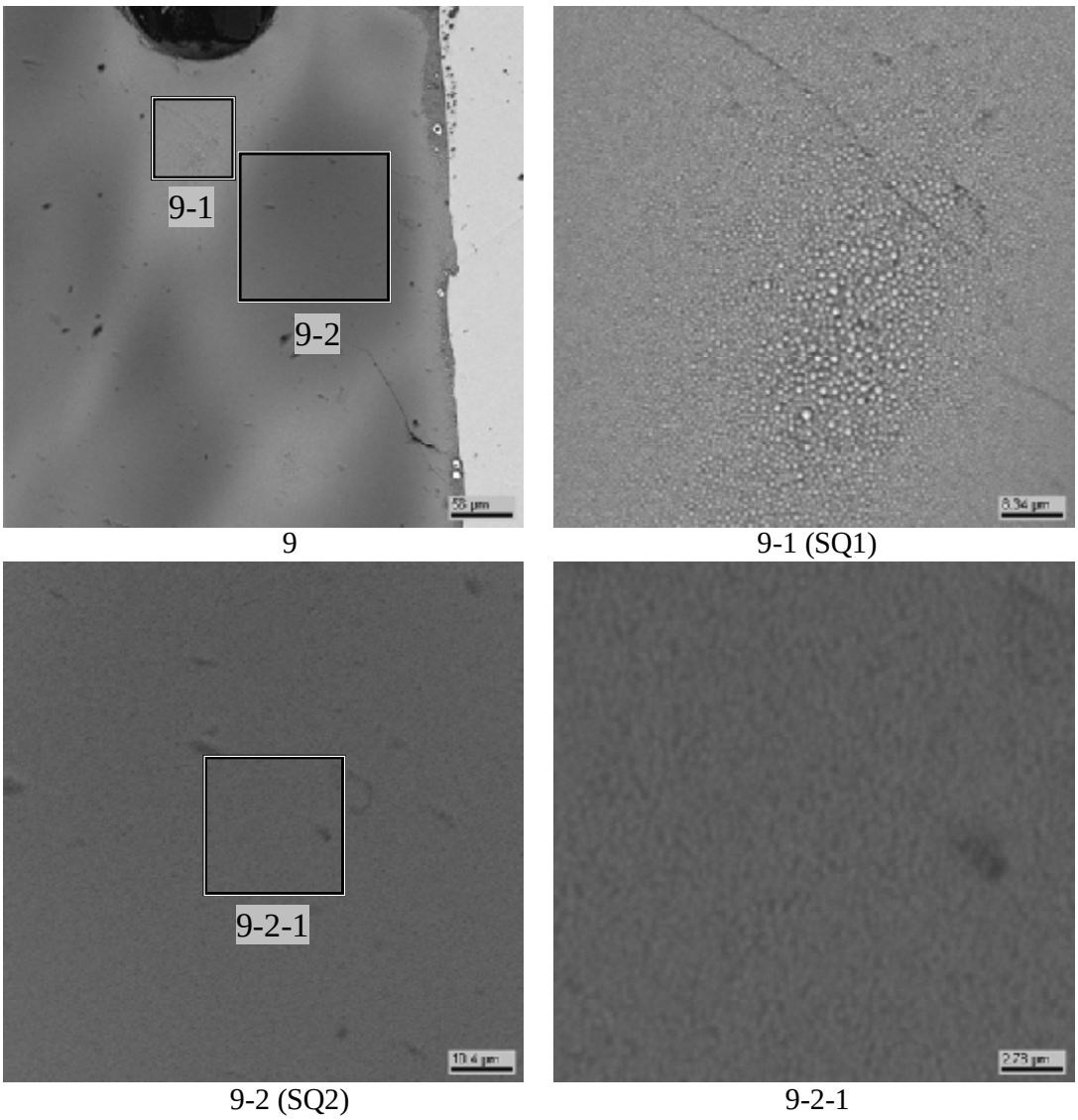

9 | 9-1 (SQ1)

9-2 (SQ2) | 9-2-1

Fig. 34. Micrographs of region 9 from the upper layer in GCord3

Table 19. Data on region 9 EDX analysis 9

No.		UO_2	SiO_2
SQ1	mass %	48.74	51.26
	mol.%	17.46	82.54
SQ2	mass %	31.77	68.23
	mol.%	9.39	90.61

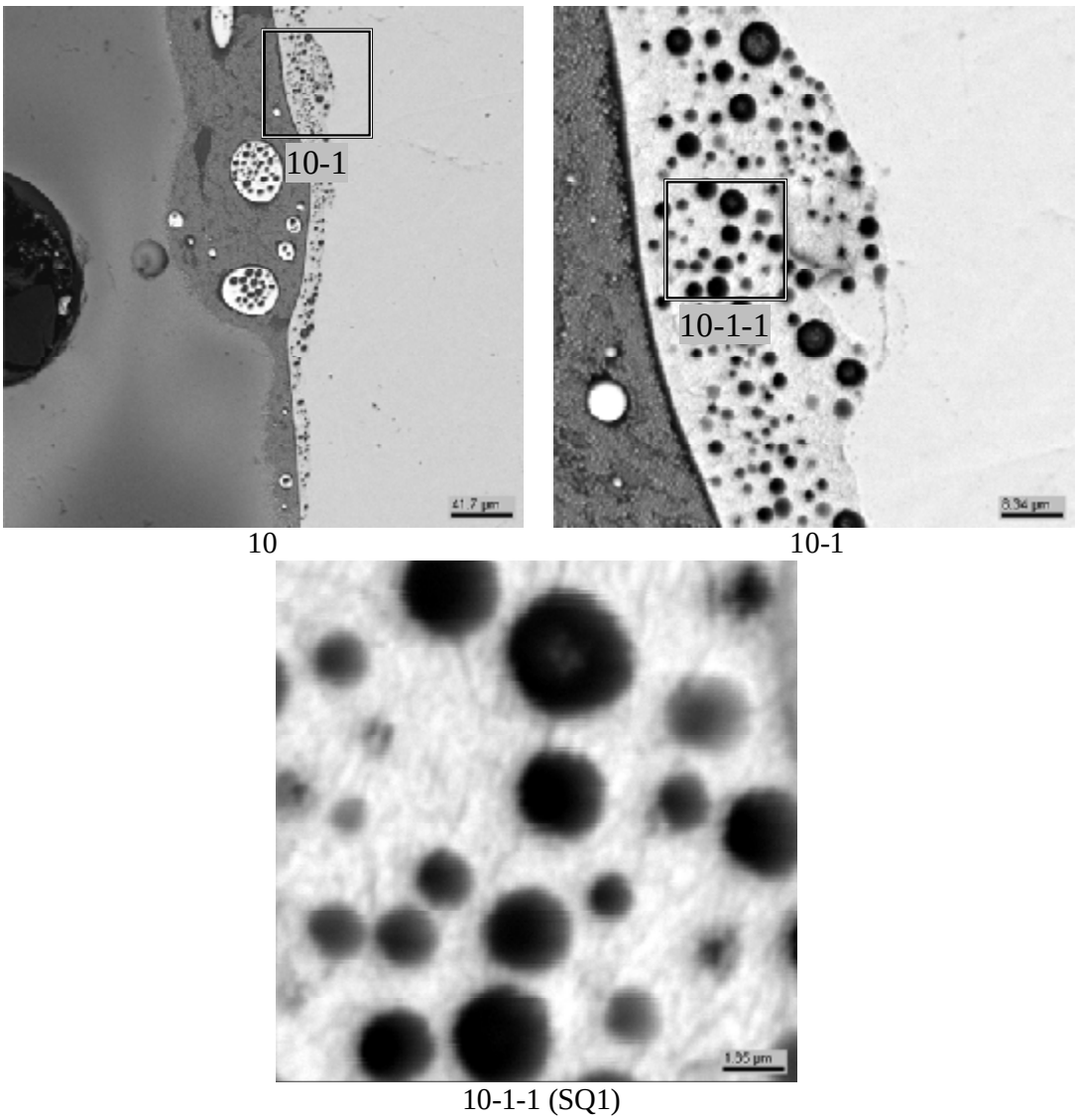

10 10-1

10-1-1 (SQ1)

Fig. 35. Micrographs of region 10 from the upper layer in GCord3

Table 20. Data on region 10 EDX analysis

No.		UO_2	SiO_2
SQ1	mass %	63.17	36.83
	mol.%	27.62	72.38

In general, like in previous tests, the upper liquid is richer in SiO_2 in comparison with the bottom liquid. It should be noted that at this temperature the upper liquid contains a smaller number of rounded inclusions with a composition similar to that of the bottom liquid. This may be due to a lesser density of the stratified melt upper layer, if compared with the previous test GCORD5 performed at a lower temperature (2080°C). Under the present conditions, most fragments of the bottom liquid have enough time to descend to the crucible bottom.

GCord4

Fig. 36 presents a SEM image of the longitudinal section of the molybdenum crucible with specimen subjected to thermal treatment at 2200°C with subsequent quenching.

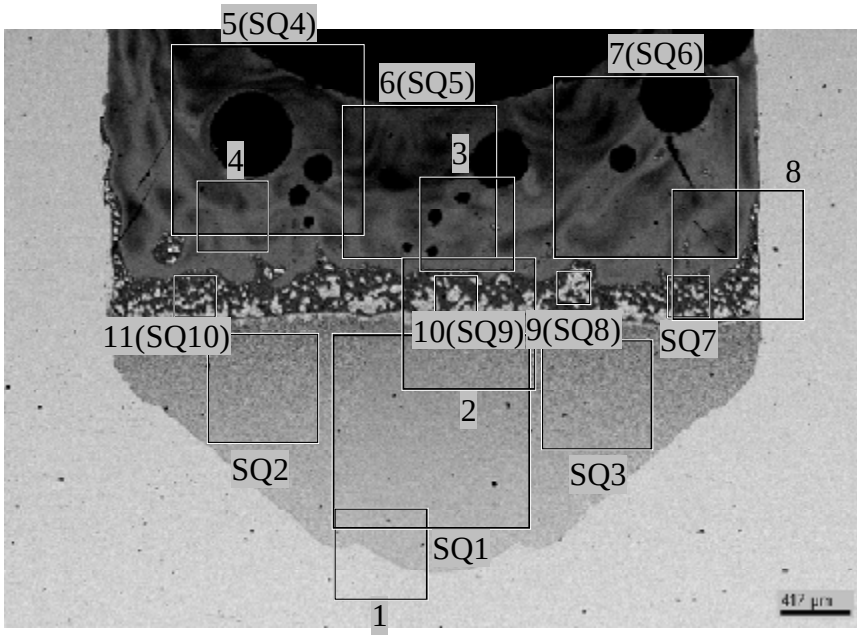

Fig. 36. SEM image for the longitudinal section of the crucible with regions marked for SEM/EDX analysis (GCord4, 2200°C)

The figure demonstrates melt stratification into two layers, the upper and bottom ones. The upper layer features a large number of big pores.

Tab. 21 contains contains the results of analysis of different regions of the section in question, from both the bottom layer (SQ1-SQ3) enriched in UO_2, the upper one (SQ4-SQ6) enriched in SiO_2, and the regions (SQ7-SQ10) at the boundary between the two layers.

Table 21. EDX data for the longitudinal section of the crucible in GCord4

No.		UO_2	SiO_2
SQ1	mass %	66.68	33.32
	mol.%	30.81	69.19
SQ2	mass %	63.56	36.44
	mol.%	27.96	72.04
SQ3	mass %	62.82	37.18
	mol.%	27.32	72.68
SQ4	mass %	39.00	61.00
	mol.%	12.45	87.55
SQ5	mass %	38.14	61.86
	mol.%	12.06	87.94
SQ6	mass %	42.27	57.73
	mol.%	14.01	85.99
SQ7	mass %	50.59	49.41
	mol.%	18.56	81.44
SQ8	mass %	55.62	44.38
	mol.%	21.81	78.19
SQ9	mass %	49.81	50.19
	mol.%	18.09	81.91
SQ10	mass %	49.25	50.75
	mol.%	17.76	82.24

Figs. 37-45 show in succession fragments of the bottom liquid, boundary region, and the upper liquid, while Tabs. 22-27 offer the corresponding EDX data for both regions and points.

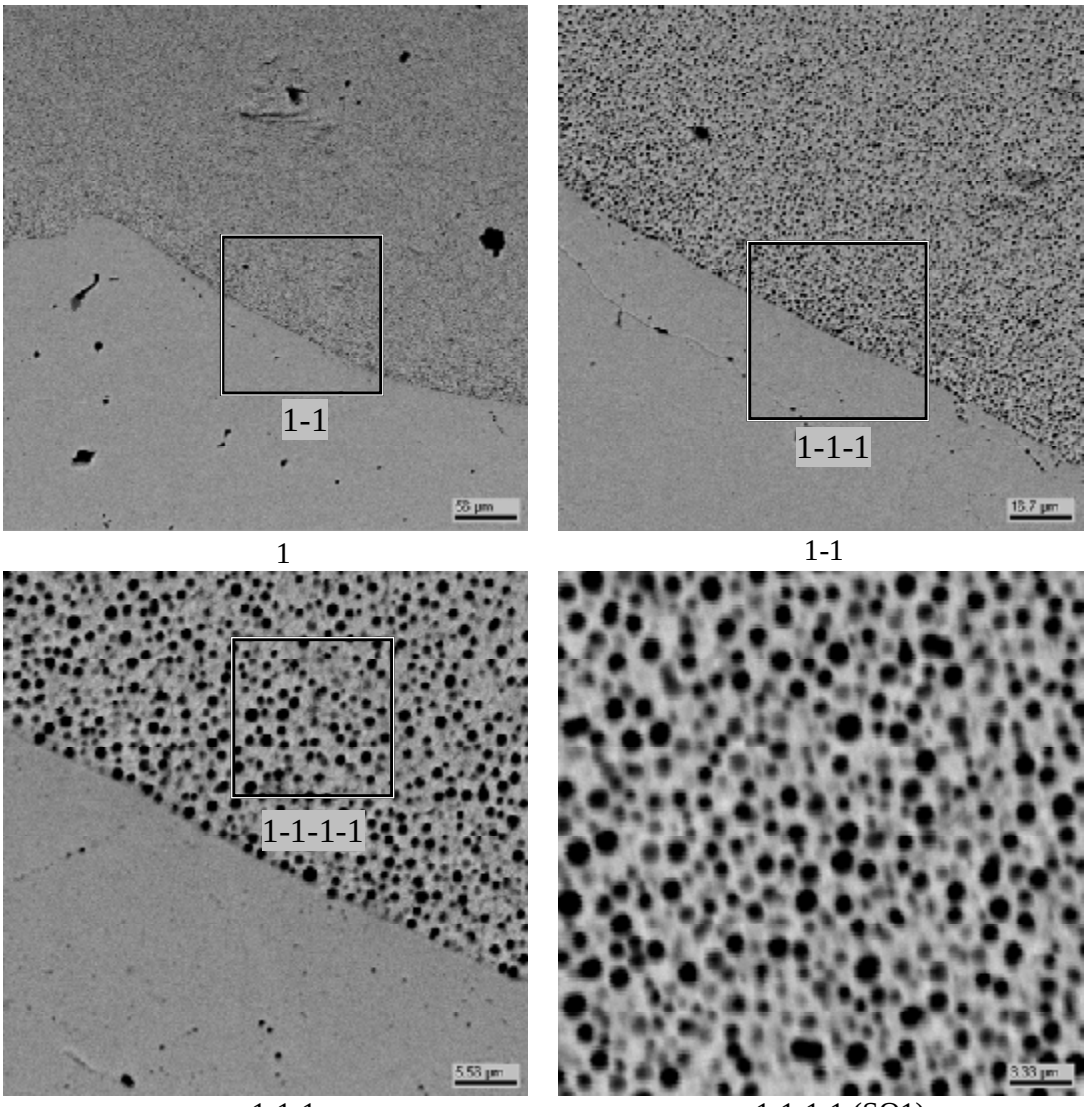

1 1-1

1-1-1 1-1-1-1 (SQ1)

Fig. 37. Micrographs of region from the bottom layer in GCord4

Table 22. Data on region 1 EDX analysis

No.		UO_2	SiO_2
SQ1	mass %	65.89	34.11
	mol.%	30.06	69.94

Note, that in this test the majority of rounded formations with a composition similar to that of the bottom liquid is concentrated in the boundary region between two layers of the stratified melt.

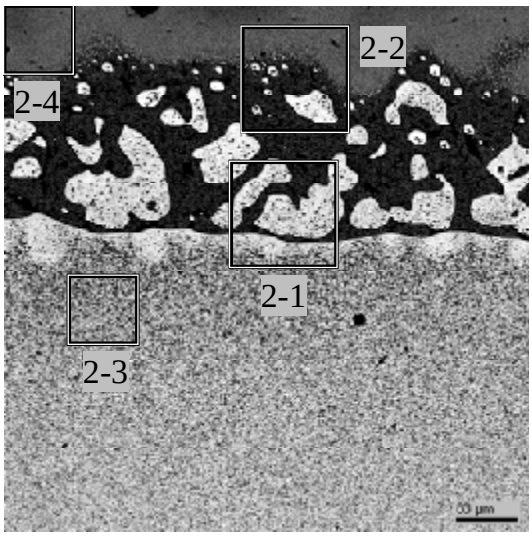

2

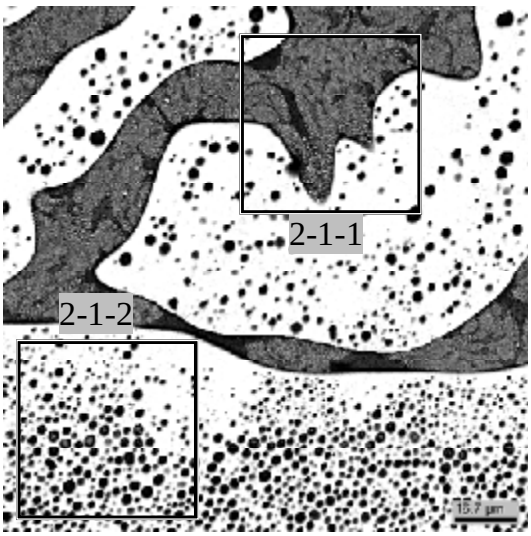

2-1

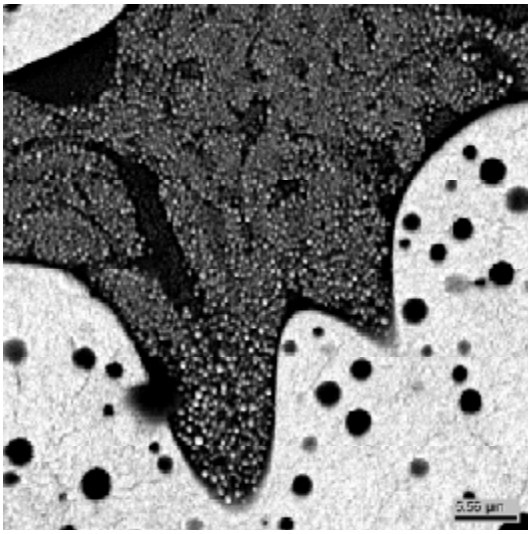

2-1-1

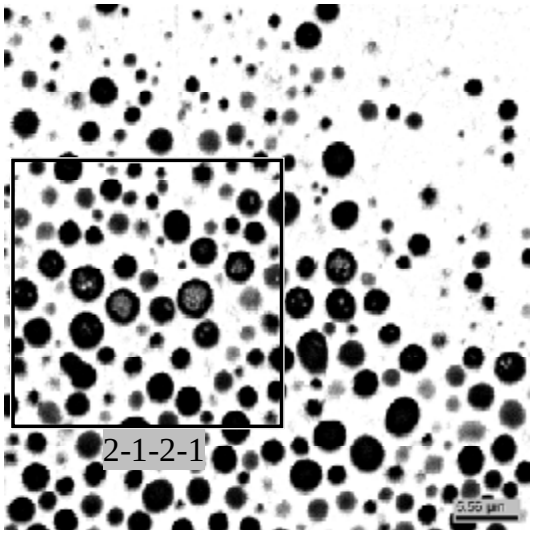

2-1-2

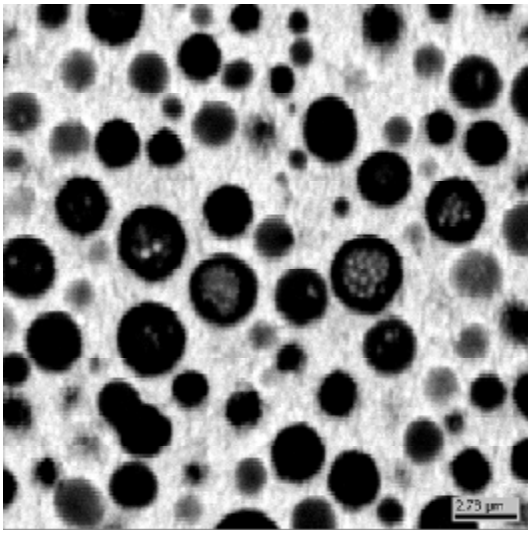

2-1-2-1

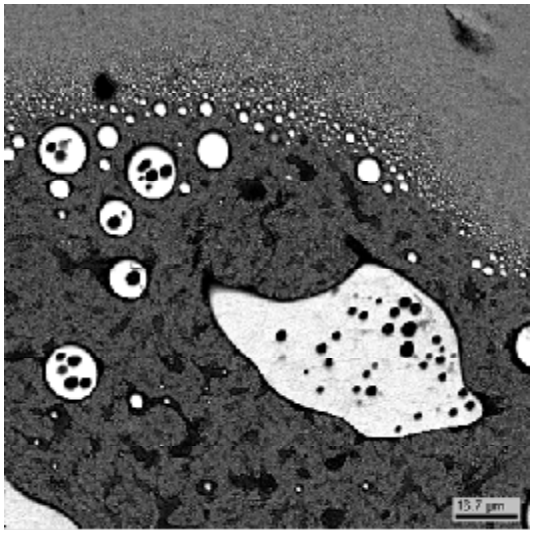

2-2

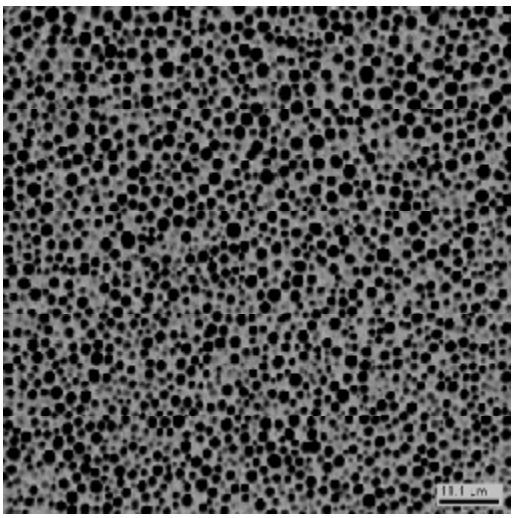

2-3(SQ1)

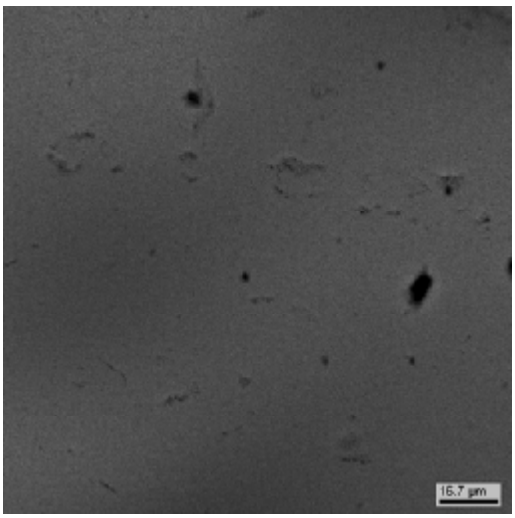

2-4 (SQ2)

Fig. 38. Micrographs of fragment 2 from the boundary region in GCord4

Table 23. Data on region 2 EDX analysis

No.		UO_2	SiO_2
SQ1	mass %	58.91	41.09
	mol.%	24.18	75.82
SQ2	mass %	45.63	54.37
	mol.%	15.74	84.26

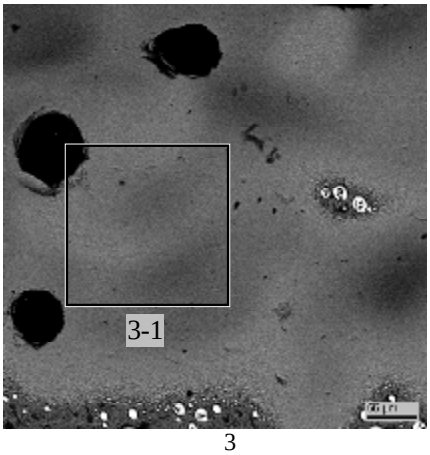

3

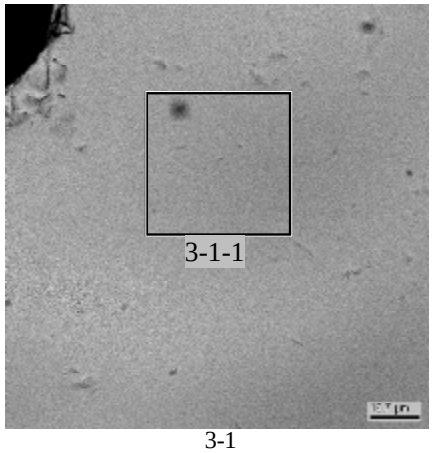

3-1

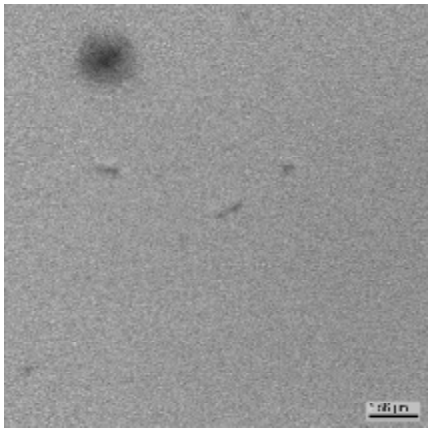

3-1-1

Fig. 39. Micrographs of region 3 from the upper layer in GCord4

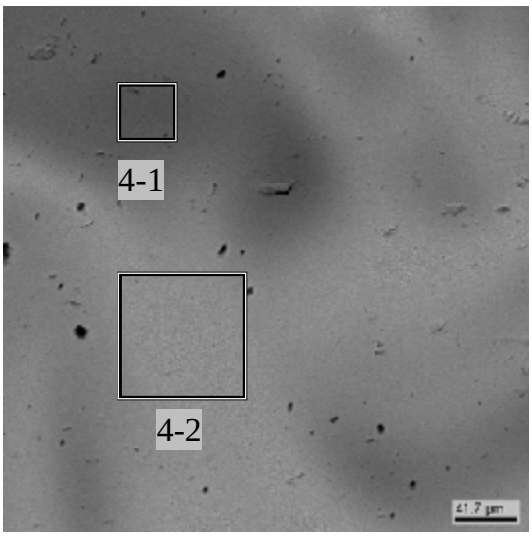

4 (SQ1)

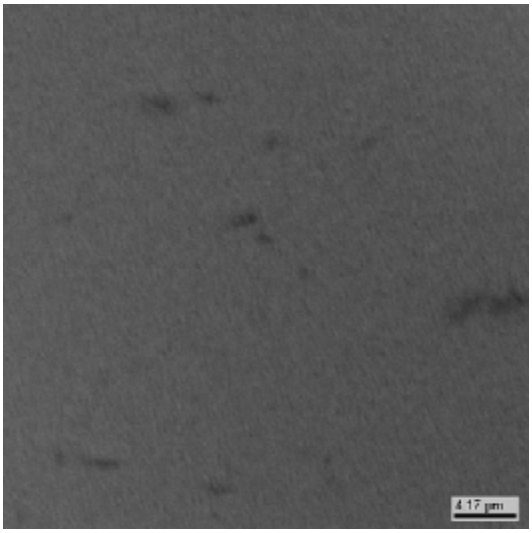

4-1 (SQ2)

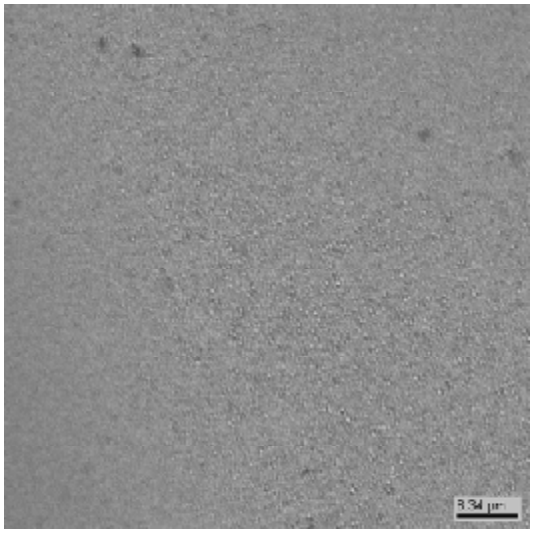

4-2 (SQ3)

Fig. 40. Micrographs of region 4 from the upper layer in GCord4

Table 24. Data on region 4 EDX analysis

No.		UO_2	SiO_2
SQ1	mass %	44.54	55.46
	mol.%	15.16	84.84
SQ2	mass %	49.60	50.40
	mol.%	17.96	82.04
SQ3	mass %	35.95	64.05
	mol.%	11.10	88.90

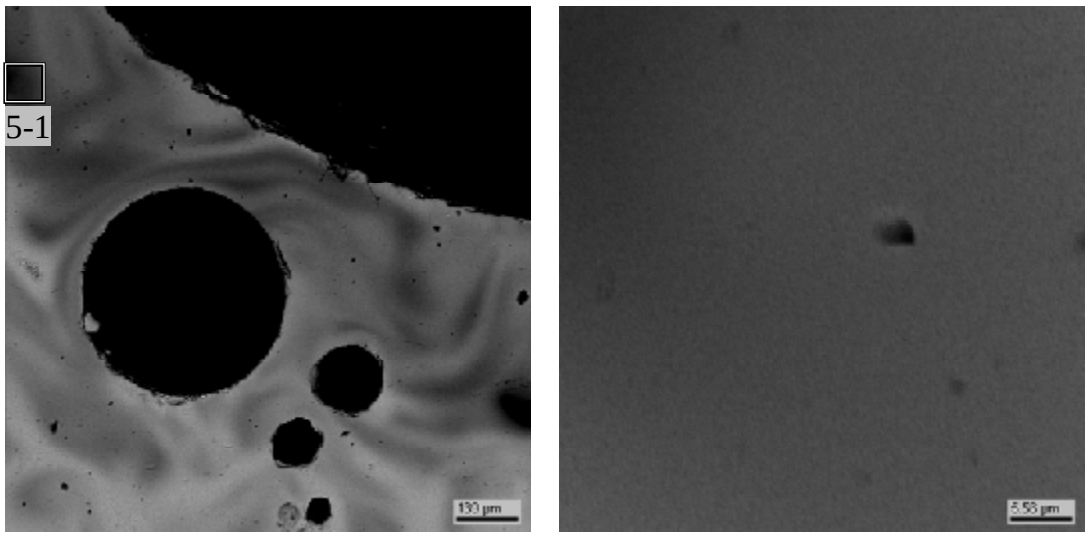

5 (SQ1) 5-1 (SQ2)

Fig. 41. Micrographs of region 5 from the upper layer with big pores in GCord4

Table 25. Data on region 5 EDX analysis

No.		UO_2	SiO_2
SQ1	mass %	39.00	61.00
	mol.%	12.45	87.55
SQ2	mass %	22.43	77.57
	mol.%	6.05	93.95

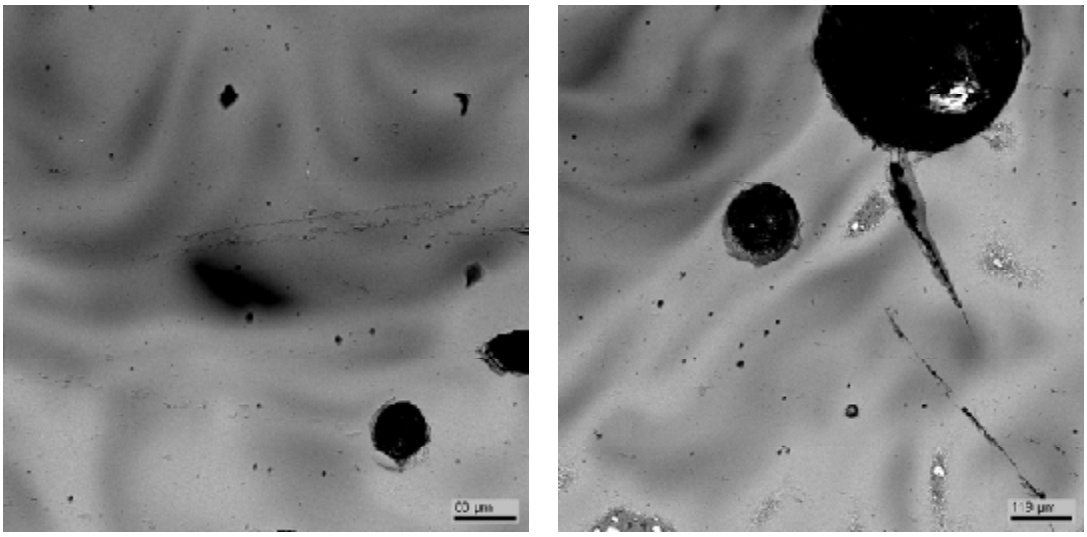

6 (SQ1) 7 (SQ2)

Fig. 42. Micrographs of regions 6 & 7 from the upper layer with pores in GCord4

Table 26. Data on regions 6 & 7 EDX analysis

No.		UO_2	SiO_2
SQ1	mass %	38.14	61.86
	mol.%	12.06	87.94
SQ2	mass %	42.27	57.73
	mol.%	14.01	85.99

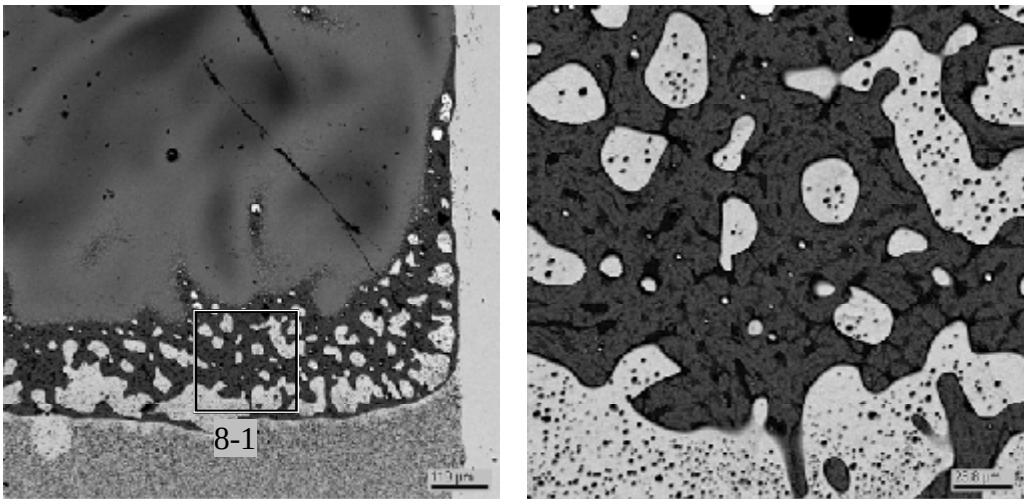

8 8-1 (SQ1)

Fig. 43. Micrographs of region 8 from the upper layer and boundary region in GCord4

Table 27. Data on region 8 EDX analysis

No.		UO_2	SiO_2
SQ1	mass %	50.59	49.41
	mol.%	18.56	81.44

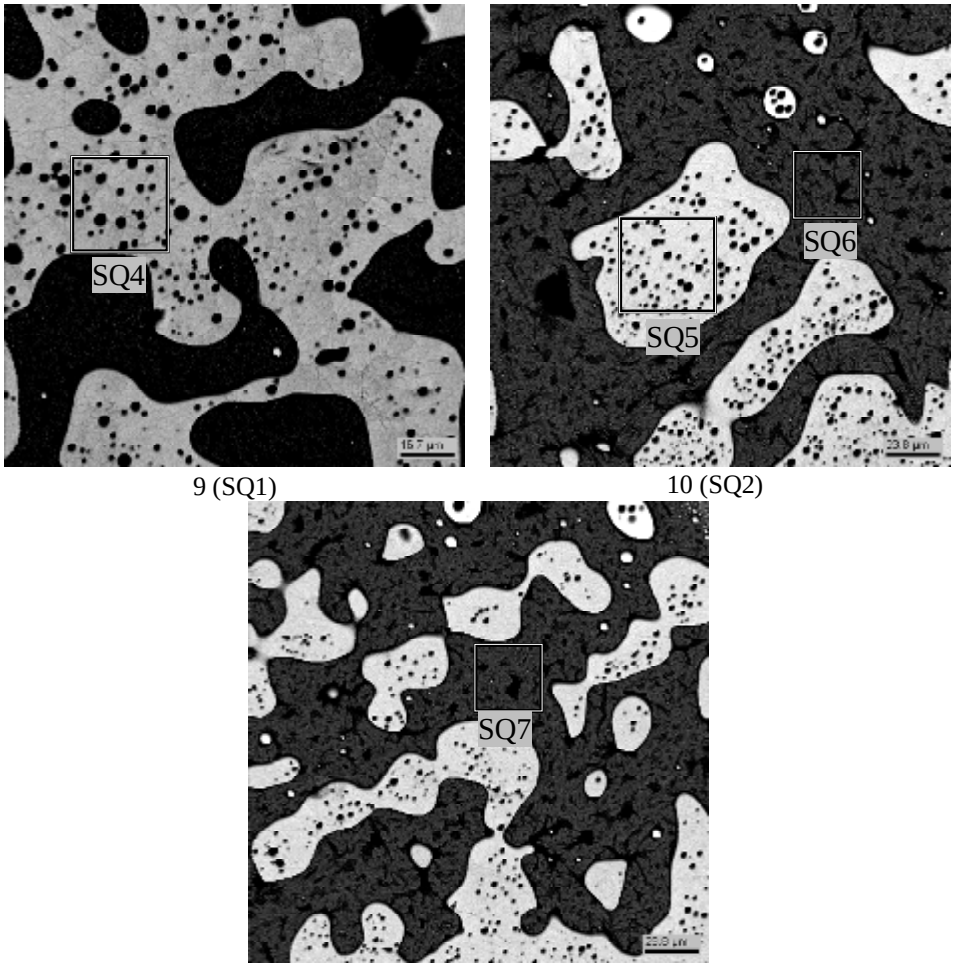

9 (SQ1) 10 (SQ2)

11 (SQ3)

Fig. 44. Micrographs of regions 9-11 from the boundary region in GCord4

Table 28. Data on regions 9-11 EDX analysis

No.		UO_2	SiO_2
SQ1	mass %	55.62	44.38
	mol.%	21.81	78.19
SQ2	mass %	49.81	50.19
	mol.%	18.09	81.91
SQ3	mass %	49.25	50.75
	mol.%	17.76	82.24
SQ4	mass %	70.11	29.89
	mol.%	34.29	65.71
SQ5	mass %	67.43	32.57
	mol.%	31.53	68.47
SQ6	mass %	38.76	61.24
	mol.%	12.35	87.65
SQ7	mass %	38.75	61.25
	mol.%	12.34	87.66

It can be stressed another time here that the light-coloured rounded formations with a composition similar to that of the segregated bottom layer (Tab. 28, SQ4, SQ5) are concentrated mostly in the boundary region (Fig. 38, 43, 44). Practically none of them were observed in the upper layer. The possible reasons may be 1) a decreased viscosity of the SiO_2-rich upper layer, which lets the rounded formations sink to the crucible bottom quicker, or 2) the secondary stratification of the melt at cooling. At this, the merging of the newly formed droplet-inclusions into globules of a larger size may be observed.

The presence of pores in the upper layer of the stratified melt and their absence in the bottom one in all tests may be linked with oxygen repartitioning between the two interacting components, i.e. UO_2 and SiO_2. Both phases can lose oxygen when temperature increases, but since the oxygen nonstoichiometry area characteristic of SiO_2 is significantly smaller than that characteristic of UO_2, then the decreasing temperature will cause the release of SiO in gaseous form from the SiO_{2-x}-rich melt in accordance with the reaction:

$$SiO_{2-x} \rightarrow SiO_2 + SiO$$

and formation of cavities, i.e. pores in the upper layer. The bottom layer contains more UO_2 than the upper one, and therefore the compensation of oxygen shortage proceeds at the expense of nonstoichiometry of UO_2 without SiO formation.

GCord9

Fig. 45 offers a SEM image of the longitudinal section of the molybdenum crucible with specimen subjected to thermal treatment at 2400°C with subsequent quenching.

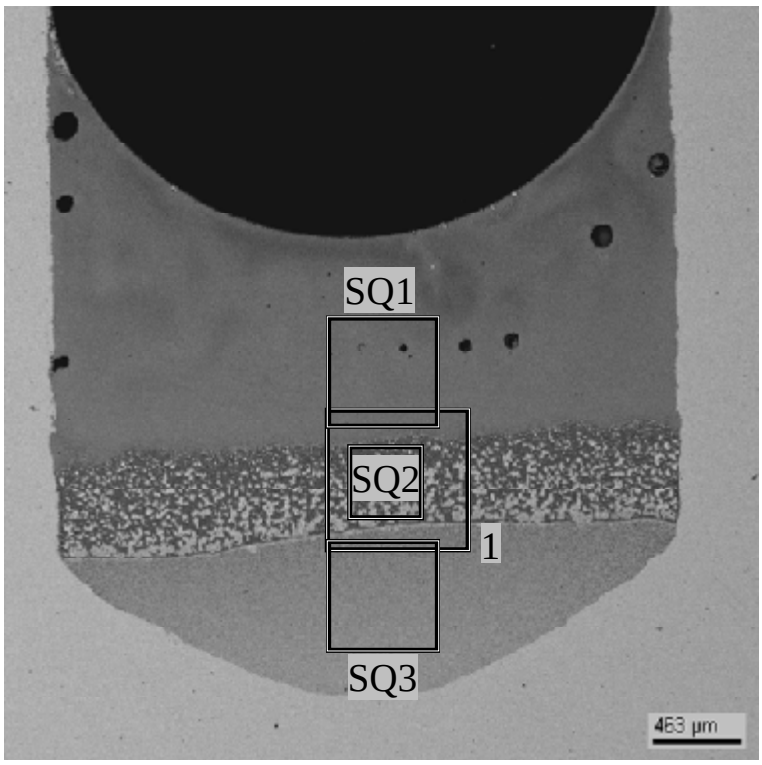

Fig. 45. SEM image of the longitudinal section of the crucible in GCord9 (2400°C) with regions marked for SEM/EDX analysis

The figure demonstrates melt stratification into two layers, the upper and bottom ones. In this case, the upper layer contains few big pores.

Tab. 29 contains the results of analysis of different regions of the section in question, from both the bottom layer (SQ3) enriched in UO_2 in comparison with other regions, the upper layer (SQ1) enriched in SiO_2, and from the boundary region (SQ2) between the two layers.

Table 29. EDX analysis data for the regions marked in Fig. 45

No.		UO_2	SiO_2
SQ1	mass %	48.44	51.54
	mol.%	17.29	82.71
SQ2	mass %	50.77	49.21
	mol.%	18.67	81.33
SQ3	mass %	62.85	37.13
	mol.%	27.36	72.64

Fig. 46 shows the boundary region between two layers in more detail

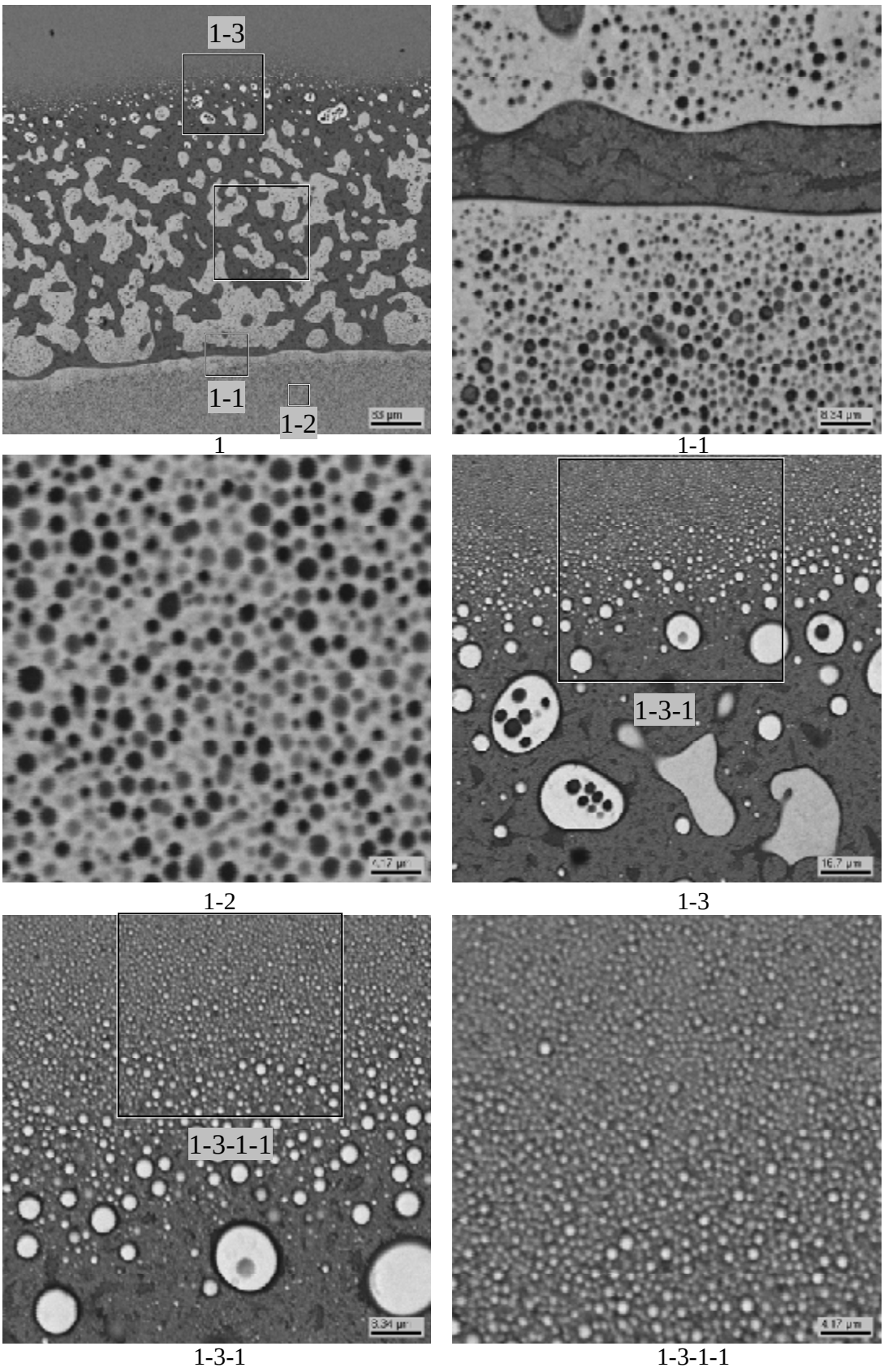

Fig. 46. Micrographs of fragment 1 from the boundary region in GCord9

At this temperature, the upper layer contains no rounded formations and has practically no pores which were characteristic of the previous tests performed at lower temperatures.

The absence of rounded inclusions in the upper liquid in GCord9 may be due to a

decreased viscosity of the SiO_2-rich melt at temperature raising up to 2400°C (compare with previous tests GCord1-4 performed at lower temperatures: 2140 and 2200°C). The result is a higher precipitation rate of the UO_2-rich melt.

2.4. Discussion of results

The analyzed results of tests with specimens having the same initial composition (18.62 mol. % UO_2 – 81.38 mol. % SiO_2) lead to generalizations given below.

Firstly, all specimens, with exception for the one quenched from 2000°C, indicated density stratification of the melt.

Secondly, light-coloured rounded formations with a composition similar to that of the bottom layer, were observed in the upper layer and boundary region. Presumably, their appearance was due to a high density of the upper stratified layer, which prevented fragments of a heavier, UO_2-rich liquid to sink to the crucible bottom. Viscosity decreases with rising temperature, therefore no light-coloured rounded globules were observed in the upper layer at 2400°C.

All EDX data for the analyzed regions of the bottom and upper liquids from each test that showed stratification are summarized in Tabs. 30 and 31.

Table 30. Summarized EDX data for the bottom layer in specimens of the UO_2–SiO_2 system

GCord	T, °C	Region or point	Composition, mol. %		Note
			UO_2	SiO_2	
5	2080	SQ1	31.76	68.24	Tab. 12
		SQ2	32.44	67.56	
		SQ3	31.57	68.43	
3	2140	SQ1	35.55	64.45	Tab. 16
		SQ2	36.17	63.93	
		SQ3	36.34	63.66	
4	2200	SQ1	30.81	69.19	Tab. 21
		SQ2	27.96	72.04	
		SQ3	27.32	72.68	
		SQ1	30.06	69.94	Tab. 22
		SQ1	24.18	75.82	Tab. 23
9	2400	SQ3	27.36	72.64	Tab. 29

Table 31. Summarized findings for the upper layer in specimens of the UO_2-SiO_2 system

GCord	T, C	Region or point	Composition, mol. %		Note
			UO_2	SiO_2	
5	2080	SQ4, SQ1	14.66	85.34	Tabs. 12, 14
		SQ5	14.40	85.60	Tab. 12
		SQ5	7.94	92.06	Tab. 12
		SQ2	8.20	91.80	Tab. 14
		SQ3	9.13	90.87	
		SQ4	8.32	91.68	
3	2140	SQ4	13.06	86.94	Tab. 16
		SQ5	10.30	89.70	
		SQ6	11.20	88.80	
		SQ7	8.05	91.95	
		SQ8	7.84	92.16	
		SQ1	11.64	88.36	Tab. 17
		SQ1	17.46	82.54	Tab. 19
4	2220	SQ2	9.39	90.61	Tab. 21
		SQ4	12.45	87.55	
		SQ5	12.06	87.94	
		SQ6	14.01	85.99	
		SQ8	21.81	78.19	
		SQ9	18.09	81.91	
		SQ2	15.74	84.26	Tab. 23
		SQ1	15.16	84.84	Tab. 24
		SQ2	17.96	82.04	
		SQ3	11.10	18.90	
		SQ1	12.45	87.55	Tab. 25
		SQ2	6.05	93.95	
		SQ1	12.06	87.94	Tab. 26
		SQ2	14.01	85.99	
		SQ6	12.35	87.65	Tab. 28
		SQ7	12.34	87.66	
9	2400	SQ1	17.29	82.71	Tab. 29

On the basis of the tabulated data, a binodal has been outlined for the miscibility gap in the UO_2-SiO_2 system (Fig. 47). For the specimens that crystallized under nonequilibrium conditions (as these specimens are due to insufficient exposure and viscous upper layer), maximum values for compositions of each liquid have been mapped on the diagram. That is, these are not averaged values, but the results of single measurements. The composition relative error is 0.3 mass %, and it cannot be depicted on the diagram on the given scale.

Findings from the present study are given in comparison with the diagram by Lungu, who observed stratification in the system.

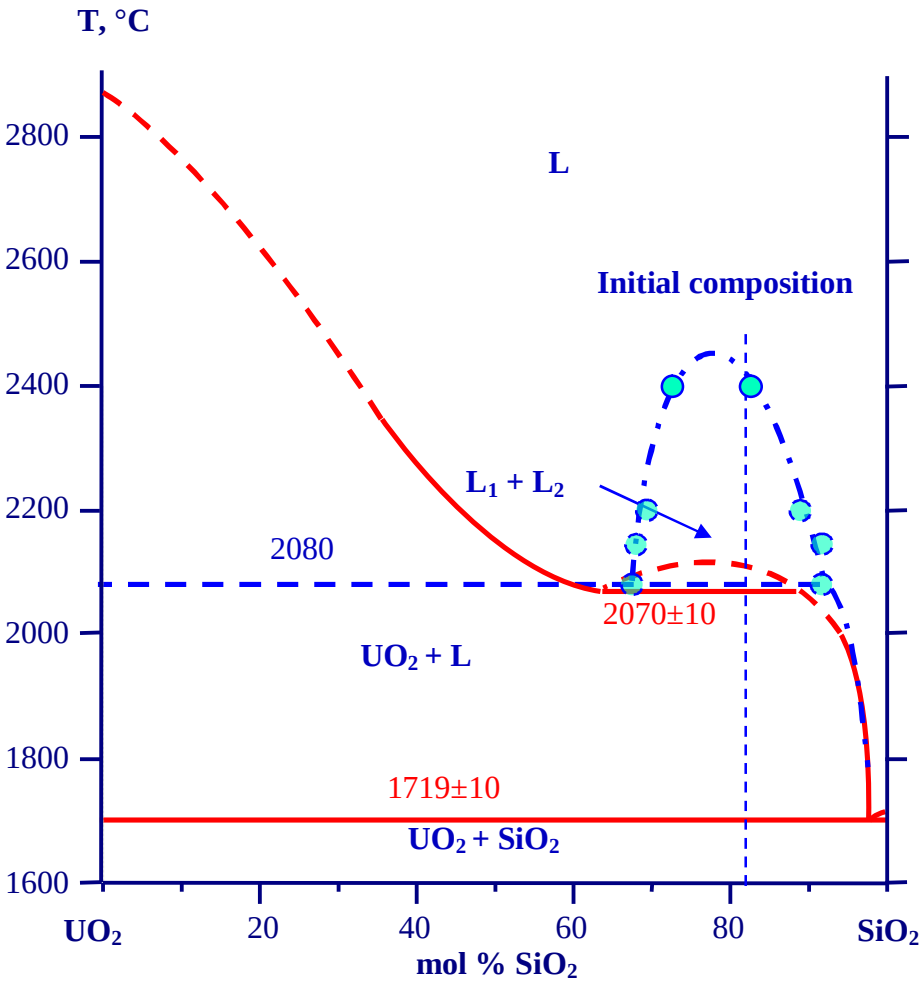

Fig. 47. Comparison of findings from this research with the Lungu's diagram [2]:
● - present research, GCord 9 data (2400°C, 1 min); ● - data from GCord2-5

2. Conclusion

The applied experimental technique makes it possible to investigate the system in question, because molybdenum does not interact with the melt throughout the temperature range of the preformed tests.

The UO_2–SiO_2 system has an extensive immiscibility gap at the SiO_2 end, which does not contradict the known Lungu's diagram [2]. Miscibility gap has been outlined using data from the performed tests.

For specifying the miscibility gap boundaries, it would be expedient to continue investigations, because the conditions close to equilibrium were achieved only in the last test at a high temperature (2400°C, GCORD9), at which low viscosity of the melt that contained over 80 mol. % SiO_2, did not prevent the coexisting liquids from attaining equilibrium concentrations.

The experimental data show the monotectic temperature to be within the 2000-2080°C range, while the binodal critical point is above 2400˚C.

References:

1. Lang S.M., Knudsen F.P., Fillmore C.L., Roth R.S. High-temperature reactions of uranium dioxide with various metal oxides. // Nat. Bur. Stand. Circular. 568. 1956. P. 1-32.
2. Lungu C.H., Revue de Physique, Roumaine Acad. Sci. 1962. V. 7. N 4. P. 419-425.
3. Galakhov F.Ya. High-temperature microfurnace for heterogeneous equilibria investigations in refractory oxide systems. – In: Modern techniques of silicate and construction materials studies. M., 1961, P 178-182. (Russ.)